AD-A014 480

CERAMIC SINTERING

Charles D. Greskovich, et al

General Electric Corporate Research and Development

Prepared for:

Office of Naval Research
Advanced Research Projects Agency

July 1975

260066

AD A014480

CERAMIC SINTERING

FINAL TECHNICAL REPORT

July 1975

Contract No.:	N00014-74-C-0331
Contractor:	General Electric Company Corporate Research and Development Schenectady, New York 12301
Principal Investigators:	Charles D. Greskovich, Joseph H. Rosolowski, and Svante Prochazka (518)346-8771 Ext. 6122/6443/6534
Scientific Officer:	A. M. Diness, ONR Code 471 Office of Naval Research Arlington, Virginia 22217
Effective Date:	April 1, 1974
Expiration Date:	August 30, 1975
Amount of Contract:	$129,787

Sponsored by

Advanced Research Projects Agency
ARPA Order No. 2698 Program Code No. 4D10

Period Covered: April 1, 1974 to June 30, 1975

This research was supported by the Advanced Research Projects Agency of the Department of Defense and was monitored by ONR under Contract No. N00014-74-C-0331.

SRD-75-084

UNCLASSIFIED

SECURITY CLASSIFICATION OF THIS PAGE *(When Data Entered)*

REPORT DOCUMENTATION PAGE		READ INSTRUCTIONS BEFORE COMPLETING FORM
1. REPORT NUMBER	2. GOVT ACCESSION NO.	3. RECIPIENT'S CATALOG NUMBER
4. TITLE *(and Subtitle)* CERAMIC SINTERING		5. TYPE OF REPORT & PERIOD COVERED Final Technical Report 4/1/74 - 6/30/75 6. PERFORMING ORG. REPORT NUMBER SRD-75-084
7. AUTHOR(s) Charles D. Greskovich Joseph H. Rosolowski Svante Prochazka		8. CONTRACT OR GRANT NUMBER(s) N00014-74-C-0331
9. PERFORMING ORGANIZATION NAME AND ADDRESS General Electric Company Corporate Research and Development Schenectady, New York 12301		10. PROGRAM ELEMENT, PROJECT, TASK AREA & WORK UNIT NUMBERS ARPA Order No. 2698 Program Code No. 4D10
11. CONTROLLING OFFICE NAME AND ADDRESS Advanced Resaearch Projects Agency 1400 Wilson Blvd. Arlington, Virginia 22217		12. REPORT DATE July 1975 13. NUMBER OF PAGES ~~88~~ 101
14. MONITORING AGENCY NAME & ADDRESS*(if different from Controlling Office)* Office of Naval Research 800 North Quincy St. Arlington, Virginia 22217		15. SECURITY CLASS. *(of this report)* Unclassified 15a. DECLASSIFICATION/DOWNGRADING SCHEDULE

16. DISTRIBUTION STATEMENT *(of this Report)*

APPROVED FOR PUBLIC RELEASE;
DISTRIBUTION UNLIMITED

17. DISTRIBUTION STATEMENT *(of the abstract entered in Block 20, if different from Report)*

18. SUPPLEMENTARY NOTES

19. KEY WORDS *(Continue on reverse side if necessary and identify by block number)*

Sintering, Grain Growth, Silicon Carbide, Silicon, Silicon Nitride

20. ABSTRACT *(Continue on reverse side if necessary and identify by block number)*

Measurement of the rate of oxidation and creep rate in air of chemically vapor deposited Si_3N_4 at around 1500°C are reported. Attempts to prepare pure, dense Si_3N_4 bodies by hot pressing powder at ultra-high pressures were partially successful.

Resistance heaters made of dense, sintered SiC were tested and found to have in-use lifetimes at least 10 times longer than those of commercially

(continued on reverse side)

DD FORM 1 JAN 73 1473 EDITION OF 1 NOV 65 IS OBSOLETE

UNCLASSIFIED

SECURITY CLASSIFICATION OF THIS PAGE *(When Data Entered)*

20.

available heaters tested in the same way. It was found that the resistivity of B containing dense, sintered β-SiC could be changed through compensation of the B acceptors by N donors introduced from the sintering furnace atmosphere during firing. The thermal EMF of a junction made of p- and n-types of dense sintered β-SiC was measured over the temperature range from 100°C to 1500°C and found to be 0.95 volt at 1500°C.

A way was found to densify B_4C without hot pressing. Bodies of B_4C having about 94% of theoretical density were made by using conventional sintering processes and doping the powder with either SiC or Be_4C.

Generalizing from the extensive work presented herein on the sintering of covalently bonded solids (β-SiC, Si, α-Si_3N_4, AlN), the following tentative conclusions may be made and serve as working hypotheses to guide further work:

1) Covalent solids are not intrinsically unsinterable.
2) Powder compacts of these materials may be caused to shrink macroscopically if -
   a. growth of second phase grains having a high aspect ratio is avoided
   b. an ultra-fine particle size is used, or
   c. an additive is employed which slows down surface diffusion so that there is a high proportion of matter flow by volume or grain boundary diffusion compared to surface diffusion.

TABLE OF CONTENTS

FOREWORD

This research was sponsored by the Advanced Research Projects Agency and carried out in the Physical Chemistry Laboratory of the General Electric Corporate Research and Development Center under U.S. Navy Contract N00014-74-C-0331 entitled "Ceramic Sintering".

The work was performed during the period April 01, 1974 to June 30, 1975.

The authors gratefully acknowledge the ceramic processing skill of Mr. C. Bobik and Mr. C. O'Clair and the contribution of Dr. R. C. DeVries and Mr. J. F. Fleischer to the hot pressing studies, as well as the assistance of Dr. C. A. Johnson with the creep studies. The authors also thank Mrs. M. Gill for the excellent SEM work.

SUMMARY

The results of measurements of the creep and oxidation rate of a pure, dense Si_3N_4 ceramic in the form of a coarsely crystalline deposit formed by chemical vapor deposition are reported. No creep deflection was observed in a sample tested in 3 point bending after 198 hours at 1560°C and with an outer fiber stress of 10,000 psi. An upper limit for the creep rate under these conditions of 1.6×10^{-7} hr^{-1} was deduced from this observation. This value is several orders of magnitude less than that expected for either reaction sintered or hot pressed, MgO doped Si_3N_4 under these conditions based on extrapolations from published data.

The oxidation rate at 1550°C in air was determined to be such as to produce a weight change of less than about 0.01 $mg/cm^2 - hr^{\frac{1}{2}}$. This upper limit is about equal to the average rate of oxidation over 100 hours at 1100°C of hot pressed Si_3N_4 doped with MgO. It is probably also very much less than the oxidation rate of porous, reaction sintered Si_3N_4, which has only been observed qualitatively.

Attempts made to produce pure, dense, fine grained Si_3N_4 by hot pressing at ultra-high pressures were ultimately successful, but the samples were not large enough to be used for creep measurements as was intended.

Resistance heater elements made of dense, sintered, boron doped SiC were made and tested. When run so that the peak surface temperature was cycled between room temperature and 1600°C, the elements survived up to 2544 cycles with no failures or apparent degradation of properties. All equivalent commercial SiC heater elements tested failed by a combination of cracking and surface oxidation after less than 200 cycles. These results indicate that resistance heaters made of dense SiC could be operated in air at power loadings considerably higher than those recommended for commercial heaters and would have an indefinately long lifetime in use.

Experiments were performed to determine the effect of the sintering atmosphere on the electrical resistivity of dense, sintered β-SiC containing B dopant as a sintering aid. The objective was to determine if the normally

p-type conductivity introduced by this dopant could be compensated by N introduced from the furnace atmosphere during sintering. The results showed that both n- and p-type conductivity could be produced in the ceramic, as well as a range of conductivity values, depending on the composition of the furnace atmosphere. A thermocouple was made of a junction of n- and p-type sintered β-SiC. With a cold junction temperature of 100°C, the thermal EMF of the hot junction was found to be 0.95 volt and 1500°C and 0.25 volt at 500°C.

The early stage of sintering of β-SiC powders containing carbon only, boron only, and carbon plus boron was studied by surface area and shrinkage measurements as well as by scanning electron microscopy. β-SiC powder containing 0.8 wt% C and 0.6 wt% B began to exhibit surface area reduction and densification at temperatures near 1500°C, whereas β-SiC powder containing only free carbon was characterized by a decrease in surface area at a temperature near 1250°C but no densification for temperatures up to 2000°C. The boron dopant essentially impeded surface diffusion and inhibited grain growth in silicon carbide until the initiation of the densification process. The grains developed during the sintering of boron and carbon doped β-SiC remained equiaxed at least up to 1900°C, but the grains formed during the sintering of β-SiC containing only free carbon were clustered into dense regions separated by large pores which developed in the structure.

In the absence of free carbon, sintered compacts of boron doped β-SiC powder densified only a few percent and then stopped. The grains were essentially equiaxed and small in size but the appearance of well-defined, grain boundary-solid-vapor intersections indicated that this structure was approaching geometrical equilibrium.

Measurements of density and relative grain size in bodies formed by sintering a β-SiC powder containing 0.8 wt% C and 0.6 wt% B for 1 hr at various temperatures between 1500°C and 2050°C were made. These show that for this powder, which can be sintered to 95+% of theoretical density, the grain growth and sintering kinetics are very similar to those observed when sintering oxide powders. The sintering behavior of this powder is, therefore, not atypical. An activation energy for grain growth of 80 Kcal/mol was obtained from these measurements.

Densification of a β-SiC powder containing B and C will stop if large single crystal plates of α-SiC form in the sintering body. These large plates contact each other and form an effectively rigid framework which prevents the further shrinkage of the body.

Examination of the microstructures developed when nondensifying powders of β-SiC are fired reveals that a great deal of densification occurs on a microscopic scale. The structure is composed of apparently pore-free polycrystalline regions connected to similar regions at a few points with a separating, interconnected structure of large pores. The dense regions are typically composed of 50-100 grains and formed from the coalescence of several thousand of the original, fine powder particles. Thus sintering to near theoretical density occurs on a microscopic scale (but still large in terms of the number of powder particles involved) but the densification does not extend throughout the body, so little or no shrinkage results. The dihedral angles observed at the pore-grain boundary intersections in this structure were all around 100° or greater; i.e., much larger than the minimum value of 60° required for pore closure, hence complete densification, to occur.

A nondensifying powder of β-SiC was hot pressed at 2050°C to force partial densification (79%) and the development of many interparticle necks, each of which normally contains a grain boundary. This sample was then annealed at 150°C below the hot pressing temperature in the absence of pressure. Except for a difference in the scale of grain size, the structure of the hot pressed and annealed sample was identical to that of a sample which had only been sintered at 1900°C. The considerable amount of pore and grain growth that occurred during the annealing treatment indicated the instability of the hot pressed, low density structure arising possibly from the presence of high energy grain boundaries. The shrinkage of these boundaries under the influence of tensile stresses, which arise when local densification occurs and which leads to the eventual separation of grains, could account for the observed course of microstructure development. The question that remains is why this mechanism does not prevent the development of the dense regions which are composed of a large number of grains.

Experiments performed with nondensifying powders of Si show that microstructures develop on sintering which are similar in all characteristics with those observed with β-SiC. This implies that the nonsinterability characteristic arises from the same causes in both materials. These Si powders could be made to shrink a small amount (∿4%) during sintering by the addition of 0.2 wt% C + 1.2 wt% B, but the little shrinkage that occurred seemed to depend principally on having a small average particle size. A finer pore-grain structure developed in sintered Si doped with C and B than that formed in the undoped material.

An amorphous Si powder made by thermal decomposition of silane had an average particle size of ∿600 Å and sintered to ∿98% of theoretical density in the pure state. This demonstrates that Si, too, is not intrinsically unsinterable. The addition of 0.4 wt% B to a partly amorphous Si powder with average particle size ∿0.18 μ markedly enhanced densification during sintering.

The development of microstructure during the sintering of both crystalline and amorphous Si_3N_4 powders suggests that the absence of much densification is associated with the development of acicular grains of β-Si_3N_4 in the fine-grained α-Si_3N_4 matrix which, similar to the development of α-SiC plates in the fine-grained β-SiC matrix, rigidify the structure of the body so that the necessary atomic adjustments at the grain boundaries cannot easily occur to permit shrinkage.

A way was found to sinter B_4C, a material which is now commercially densified only by hot pressing. Bodies with relative densities up to 94% were produced by the conventional sintering method by using powders to which either SiC or Be_4C were added.

LIST OF ILLUSTRATIONS

(LIST OF ILLUSTRATIONS - cont.)

(LIST OF ILLUSTRATIONS - cont.)

(LIST OF ILLUSTRATIONS - cont.)

(LIST OF ILLUSTRATIONS - cont.)

LIST OF TABLES

The principal task executed under this contract was the study of the sintering phenomenon as it occurs in covalently bonded solids. However, work was also done on a number of other tasks dealing mostly with the properties of SiC and Si_3N_4 ceramics. These will be reported on first in sections I through V. Discussion of the sintering investigations starts in section VI.

I CREEP OF CVD Si_3N_4

The investigation of creep in air of a pure, polycrystalline α-Si_3N_4 was conducted on chemically vapor deposited material made by a chemical vapor deposition (CVD) process in which $SiCl_4$ was reacted with NH_3 at 1400°C and the resultant Si_3N_4 deposited on a graphite substrate[1]. The deposit, after removal from the substrate, was measured with a micrometer and found to have a thickness of 16 mils. It was coarsely crystalline and quite rough, with single grains extending through the whole of the thickness. Its density is 99.5% of theoretical. Figure 1 is a scanning electron micrograph of the exposed surface of the deposit. The side which was against the carbon substrate does not show crystal faces.

No chemical analysis of the material is available; however, the method of its formation insures that it is considerably purer than either reaction sintered or hot pressed Si_3N_4. The optical reflectance spectrum indicates that the oxygen content is probably less than around 30 ppm. It has also been determined that there are residual stresses present in the deposit at room temperature.

Creep was measured in three-point bending. The sample was about 1 inch long by 0.2 inch wide and supported at its ends on SiC knife-edges. These rested on a SiC plate, having a hole in its center, which lay on a geometrically similar alumina plate placed in the center of a platinum wound, horizontal tube furnace of 1¼ inches i.d. Load was applied to the sample by means of a SiC "picture frame", the top side of which was a knife-edge resting across the middle of the sample. This picture frame hung down through the holes in the base plates and its bottom side fit into a slot

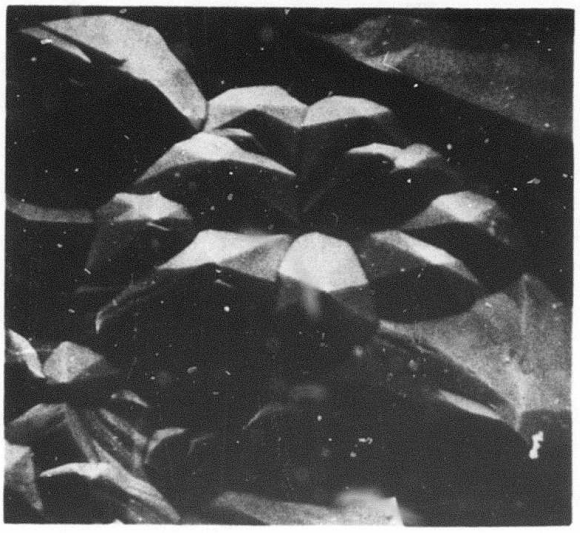

Fig. 1 Scanning electron micrograph of the exposed surface of the CVD Si_3N_4. 500X

ground into a SiC rod which passed through the wall of the furnace to the outside. A beaker attached to the end of the rod contained the loading weights. The knife-edge on the picture frame and one in the slot cut in the rod formed a universal joint which insured that the load was applied uniformly across the width of the sample (neglecting roughness).

The ends of the furnace were fitted with fused silica windows and the sample was photographed periodically. The amount of creep was determined by measuring the distance between the top of the picture frame and the point where it passes through the SiC support plate. This measurement was made on the photographic negative using an X-ray film reader which has an accuracy of 2 microns. Even without going to the trouble of enlarging the image obtained on the 35 mm film, a sample deflection of 15 microns should be readily resolvable by this technique. This corresponds to an outer fiber strain of about .01%, calculated from the formula obtained assuming that the strain rate is proportional to stress. That formula is

$$y = \frac{\varepsilon \ell^2}{6h} ,$$

where y = deflection at center of span
ε = outer fiber strain
ℓ = distance between beam supports ($\sim$.65 inch)
h = thickness of beam ($\sim$0.013 inch).

The following runs were made:

A. A sample was loaded, cold, so that the outer fiber stress was about 20,000 psi. This was calculated using the formula

$$T = \frac{3}{2} \frac{P\ell}{wh^2} ,$$

where T = stress
P = load
w = width of beam

and the other symbols have the same meanings as before. This sample remained loaded and cold over a weekend. It broke on heat-up when the temperature reached 700°C, which occurred about 20 minutes after start-up.

B. Another sample was loaded to an outer fiber stress of 5000 psi and brought up to 1400°C (2552°F). This temperature was chosen because

it is somewhat above the peak temperature expected to be encountered in gas turbines of the type for which parts made of Si_3N_4 are being considered. After 70 hours the film was developed and no creep deflection was observed.

C. With the temperature maintained at 1400°C, the loading on the sample was increased so that the outer fiber stress was 10,000 psi. After 118 hours, no creep deflection was observed.

Early in the course of this run a voltage transient on the line caused the fuse in the furnace power supply to blow during the night. The cold furnace and sample were reheated the following morning and the run was taken to start when the furnace temperature reached 1400°C again.

D. With the load maintained at 10,000 psi, the furnace temperature was raised to 1500°C (2732°F). After 92 hours no creep deflection was observed. The run was continued but the furnace winding burned out during one night. The sample was at room temperature and intact when examined at 8 a.m. the following morning but was found to have broken when examined an hour later. It is not known what caused the sample to break in this way, either during this experiment or during that described in section A above.

E. The furnace was rewound and another sample was loaded to 10,000 psi and held at 1560°C (2840°F). No creep deflection was observed after 198 hours at temperature. The furnace winding failed during the night and the sample was found to be at room temperature and broken the following morning.

These results only allow an upper limit to be established for the creep rate. Assuming that a 20 micron total sample deflection had occurred, it can be estimated that the creep rate at 1560°C and an outer fiber stress of 10,000 psi is less than about 1.6×10^{-7} hr^{-1} for the silicon nitride investigated. This value is about the same as the lowest steady state creep rate measured on reaction sintered, impure silicon nitride of around 75% of theoretical density in

experiments run in the temperature range between 1200°C and 1315°C (the highest temperature investigated) and outer fiber stresses between 10,000 psi and 20,000 psi[2]. The creep rates measured on this reaction sintered material are at least an order of magnitude less than those measured on Norton's HS-130 hot pressed silicon nitride for the same conditions[3]. Judging from the published data, one can reasonably expect that the upper limit of the creep rate given here for the CVD silicon nitride at 1560°C and 10,000 psi is many orders of magnitude less than that which would be measured for either hot pressed or reaction sintered silicon nitride under the same conditions.

II OXIDATION OF CVD Si_3N_4

Oxidation of the CVD silicon nitride was investigated by maintaining specimens at an elevated temperature in air with periodic removal from the furnace for weighing to determine the amount of SiO_2 formed. During oxidation, the specimens lay on a bed of high purity silicon nitride powder which was held in a silicon carbide boat.

The principal difficulty in the experiment arose from the fact that the surface area of the samples could not be determined. In spite of the roughness apparent in Fig. 1, the total surface area was far too small to be determined by the BET method. Accordingly, the surface area of the samples was taken to be that of smooth pieces having the same shape and a thickness of 0.013 inch. The weight increase of each sample due to oxidation was then expressed in milligrams per square centimeter and those data plotted as a function of the square root of time in hours.

Figure 2 is a plot of the data obtained in this way at 1410°C. The abscissa of every point on the true oxidation curve is, of course, obtained by dividing the abscissa of every point on the curve shown by the ratio of the actual sample area to the area assumed. It is estimated that that ratio lies between 2 and 4.

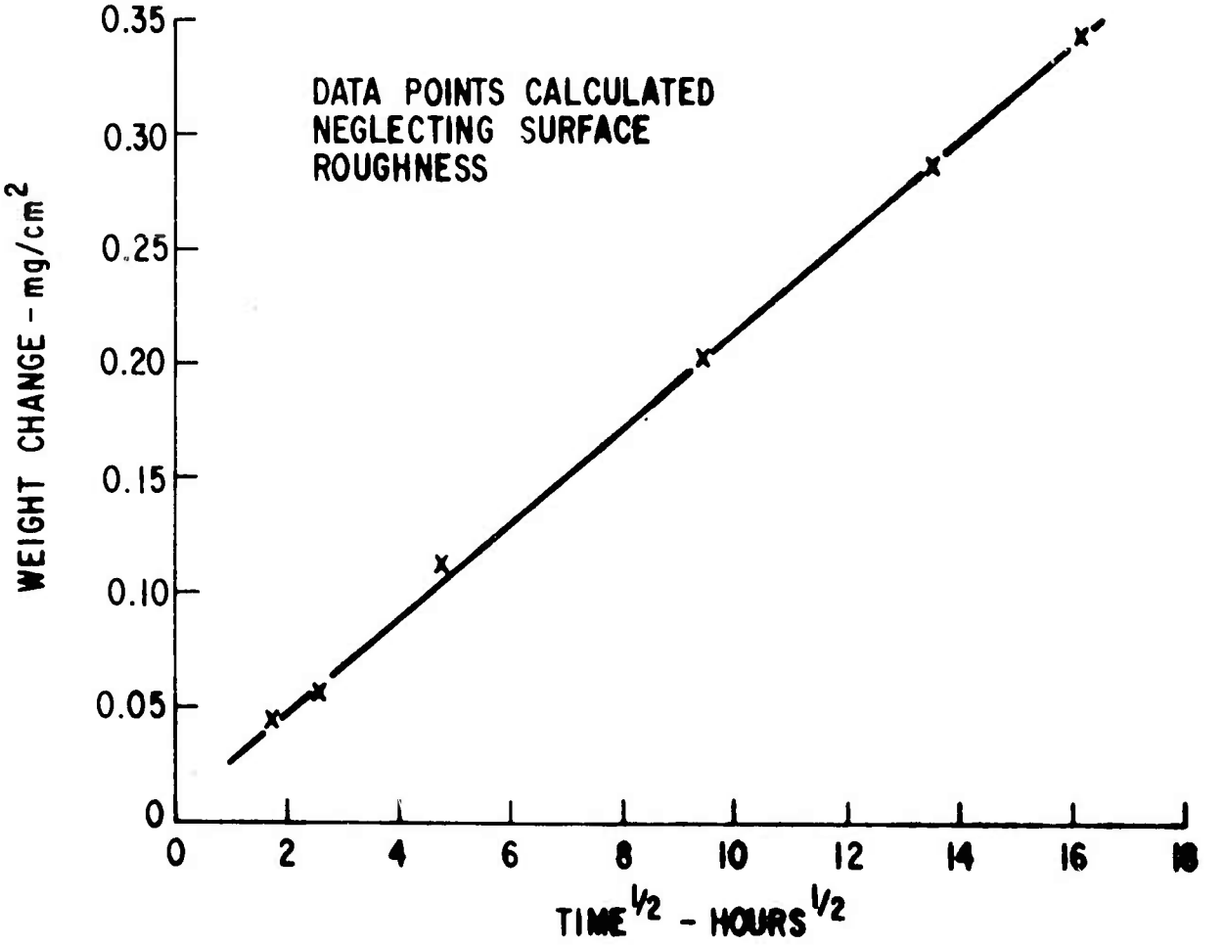

Fig. 2 Oxidation of CVD Si_3N_4 in air at 1410°C.

Figure 3 is a scanning electron micrograph of the oxidized surface of one of the samples at the end of the 1410°C run. The oxide layer, although cracked, is seen to be adherent. The oxide was determined to be α-Cristobalite. This was also the crystalline form of the oxide on the powder on which the samples lay.

Figure 4 shows oxidation data obtained at 1550°C. Comparison with the data in Fig. 3 shows that the oxidation rate at this temperature is apparently less than that at 1410°C. To check this, one of the samples used in the 1410°C run was soaked in HF to remove most of the oxide and placed in the boat with the other samples. Its rate of weight gain was significantly greater than that of the other samples as well as being greater than that which it had experienced at 1410°C. Accordingly it was concluded that the apparent decrease in oxidation rate on going from 1410°C to 1550°C probably results from a difference in the roughness (i.e. specific surface area) of the samples used in the two runs, with the samples run at 1410°C being the rougher. It may be further mentioned that the individual weight gains of the samples in each run were consistent with each other. Also, all of the samples used in a single run came from the same region of the original CVD deposit.

The oxidation rate of the CVD silicon nitride at 1550°C in air then can be taken from these data to be such as to produce a weight change of less than 0.01 $mg/cm^2 - hr^{\frac{1}{2}}$. This is considerably lower than the only other values that were found in the literature. The oxidation rate for hot pressed material containing 5 wt% MgO is given as 1 mg/cm^2 for 100 hours at 1100°C[4]. Another reference gives 0.11 $mg/cm^2 - hr^{\frac{1}{2}}$ at 1400°C for an unspecified form of silicon nitride[5]. Porous, reaction sintered material has also been qualitatively shown to have a high oxidation rate[6].

III HOT PRESSING PURE Si_3N_4

Attempts were made to produce samples of pure, dense, polycrystalline Si_3N_4, of a size suitable for measuring creep in the manner described in section I by hot pressing powder in a high pressure apparatus of the type

Fig. 3 Scanning electron micrograph of the surface of the CVD Si_3N_4 after oxidation for 259 hours in air at 1410°C. 500X

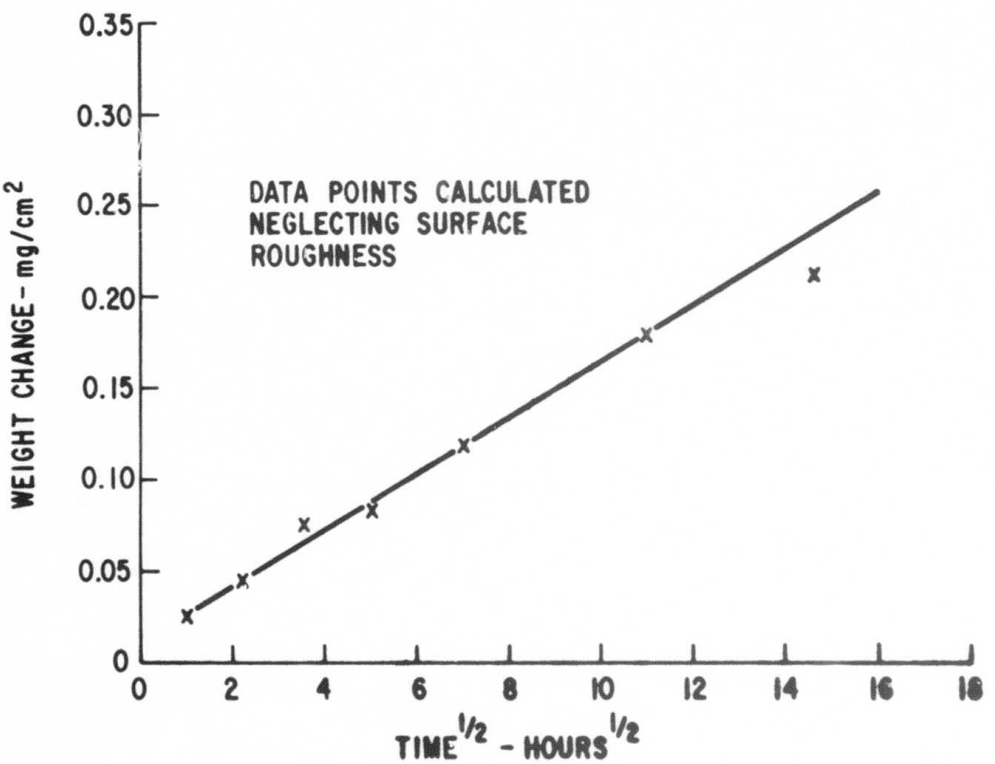

Fig. 4 Oxidation of CVD Si_3N_4 in air at 1550°C.

used in diamond synthesis. The powder used was obtained from the Plessy Co. of Frenchtown, NJ[7]. The vendor's analysis showed it to be 91% alpha Si_3N_4 and the rest beta. The impurity content, as determined spectrometrically was given as

Na, K	-	not detected
Ca	-	1-10 ppm
Al	-	100 ppm
Cu	-	10-100 ppm
Fe	-	up to 1000 ppm.

The oxygen content was given as lying between 1.3 and 1.5 weight percent and the average particle size was about 0.2 microns.

The hot pressing was done in a belt apparatus. In this technique, an essentially hydrostatic pressure is applied to a sample by placing it in the center of a cell filled with a salt which becomes plastic at high temperature and pressure. The high temperature is achieved by passing an electrical current through a hollow graphite cylinder surrounding the salt, and the pressure is generated by movable rams bearing on the ends of the cell. The sample is separated from the salt by a thin liner.

The experiments are described in more detail in the first Semi-Annual Technical Report[8]. Various runs were made using pressures between 40 and 60 kilobars, temperatures between 1200 and 1750°C, hold times between 0.5 and 4 hours and liners of Ni, Mo, Al_2O_3, C, BN powder and no liner at all. The results were disappointing because in all cases but one, there was a considerable degree of reaction of the Si_3N_4 with the liner. The exception was the case when the liner was omitted and the Si_3N_4 was in direct contact with the NaCl in the cell. In that case, however, the pressed sample had only achieved 85% of theoretical density after 4 hours of sintering. Appreciable porosity was also evident in most of the other samples. The test samples were cylinders about . mm in diameter and about 4 mm long. They tended to break up into lamellae on removal from the apparatus.

The results obtained in these experiments were not encouraging enough to engender a reasonable hope that the problems associated with making dense, pure samples of a size required for the objectives of the contract could be solved in anything like the time available. Accordingly, work in this area was terminated.

In some recent experiments using a press having a larger pressurized volume and a solid BN liner, a powder made by reacting SiH_4 with NH_3 at 700°C was pressed to 97% of theoretical density in 35 minutes at between 1500 to 1550°C and 20 kilobars of pressure. These samples showed no evidence of reaction with the liner or delamination tendency. Their maximum size (.25 in diameter × .125 in high) was, however, still too small for them to be made into creep test samples.

IV SiC RESISTANCE HEATERS

The development of a technique of producing SiC ceramic bodies of 90+% density and controlled electrical resistivity by cold pressing and sintering opens the possibility of making resistance heaters of this material. Commercial SiC resistance heaters are highly porous, coarsely crystalline bars produced by a reaction sintering technique. They are subject to oxidation when used in air, the SiO_2 thus formed reducing the contact area between grains and so increasing the resistance of the heater. This oxidation process restricts their use in air to temperatures below about 1400°C if reasonable lifetimes are to be achieved. Furthermore, it is recommended that they not be allowed to cool below about 700°C during use since cooling below that temperature leads to cracking of the oxide formed on the SiC grains thus exposing fresh surface to rapid oxidation. It was expected that a resistance heater made of dense SiC would have only a small surface area accessible to oxidation and should, therefore, last much longer in use than the currently available commercial heater.

Accordingly, rods of dense SiC having a length of 6 inches and ¼ inch in diameter were prepared by firing isostatically pressed silicon carbide powder containing boron and carbon for ½ hour at 2100°C in an argon-nitrogen atmosphere. The resulting rods were 91% dense and had an end to end room temperature resistance of about 2 ohms. The average grain size was about 4 microns. Rods of similar dimensions were prepared from commercial, ½ inch diameter SiC resistance heater rods by cutting and grinding to size.

Parallel flats were milled on the end 3/4 inch of each rod, and after copper plating indium-gallium liquid was applied. The ends were held between water cooled copper blocks which served as the heat sinks and current leads to the rods. The peak current through the rods was adjusted so that a temperature of 1600°C was achieved at the hottest point on the surface. Each rod was fully exposed to the air and the temperature was measured with an optical pyrometer.

The current through the rod was controlled so that the full current was maintained for 5 minutes. This was followed by two steps of reduction by 1/3 of the peak current. Each of these current levels was maintained for 20 seconds. On the first the peak rod surface temperature dropped to about 1250°C, and the rod surface was only faintly self-luminous on the second. This was followed by a final reduction to zero current which was maintained for 30 seconds, after which the current increased to the peak value again in a manner inverse to that by which it was decreased.

Three of the rods made of commercial material were tested. They survived 129, 147 and 192 heating and cooling cycles, respectively. Failure occurred by a crack across the bar that had an oxidized surface. The face of one such cracked surface is shown in Fig. 5. The lighter material is SiO_2, which was also present in quantity on the outside surface of the rod. Figure 6 is a micrograph of the cross section of a commercial rod sample before use. The large grain size and porosity are apparent.

Observation of these rods during testing revealed that the cracks formed many cycles before the rod finally failed to conduct current. The rigid rod supports apparently kept the pieces in contact and maintained current continuity until the crack surface became badly oxidized.

None of the dense SiC rods failed during testing. One was run for 1587 cycles and another for 2544 cycles. The only change in the latter was a decrease in its room temperature resistance; going from 2.05 ohms when the test started to 1.5 ohms when it was terminated. The peak current in both of these rods was around 30 amperes when the applied voltage was about 41 volts. The outer surface took on a yellowish color after the first few cycles which did not change appreciably thereafter. Figure 7 is a

Fig. 5 Cracked surface of a commercial SiC heater rod which failed during cyclic testing. 12X

Fig. 6 Cross section of a commercial SiC heater rod before use. 14X

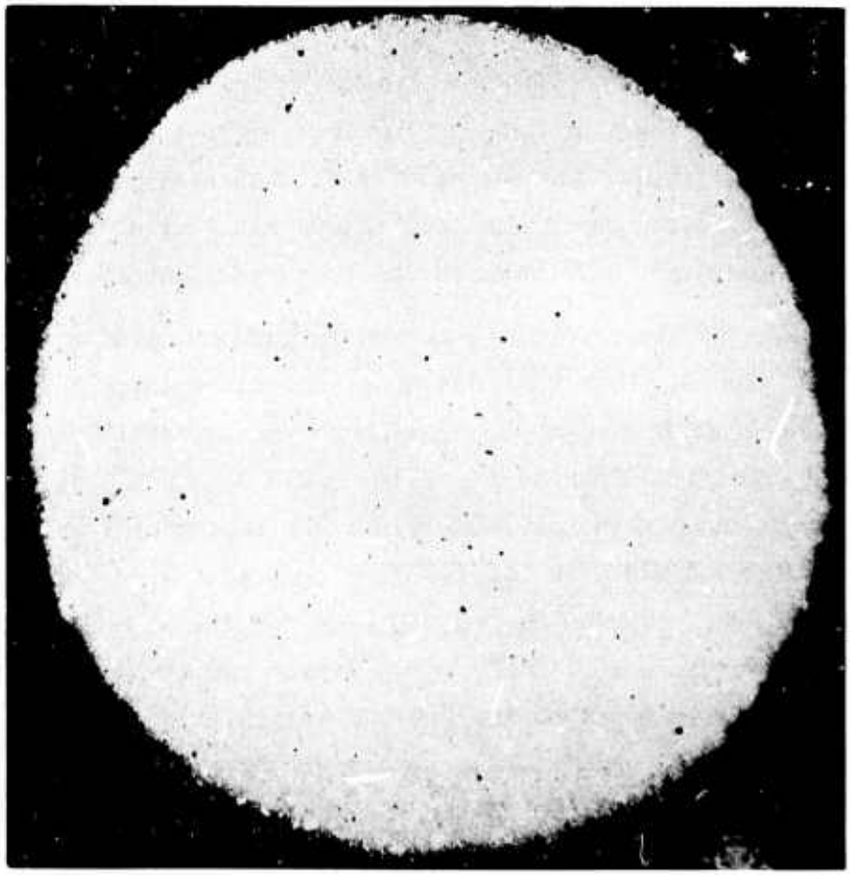

Fig. 7 Cross section of a dense Sic heater rod which had been cycled between room temperature and 1600°C 2544 times. 20X

cross section of the rod that had run for 2544 cycles. It looks no different from a pristine rod. In particular, there is no evidence of a thick oxide layer on the outer surface. There was no indication that the dense SiC rods could not have endured the test indefinately.

In the light of these results, it was decided to raise the peak surface temperature to 1700°C. When this was done, it was observed that those portions of the rod surface whose temperature was around 1630°C or higher were oxidizing rapidly. Bubbles of silica could be seen being blown out of the surface. These were initially clear but soon became opaque. In Fig. 8, the lower rod had been run for 1587 cycles at a surface temperature not exceeding 1600°C. The upper rod had been run for 10 cycles with a peak surface temperature of 1700°C. This latter rod was not uniform in resistivity along its length so the hottest region, indicated by the bubbly surface, did not occur in the center of the rod. The bubbling did not extend into the portion of the rod where the temperature was less than 1630°C.

Figure 9 is a micrograph of a cross section of the bubbly portion of the rod showing that a structural transformation had occurred. The central portion has the original structure of the rod but the surrounding material is very porous and composed of large crystals (the bright areas). Both the core and its surrounding region are composed of β-SiC. There is little oxide in the porous region; most of it is on the outside surface.

These tests indicate that resistance heaters made of dense SiC would be clearly superior to those currently offered commercially since they could be operated at higher power loadings (in watts per unit area of radiating surface) than those recommended for the commercial product and still have a very long service life. In addition, they could be cooled to room temperature after use without being adversely affected.

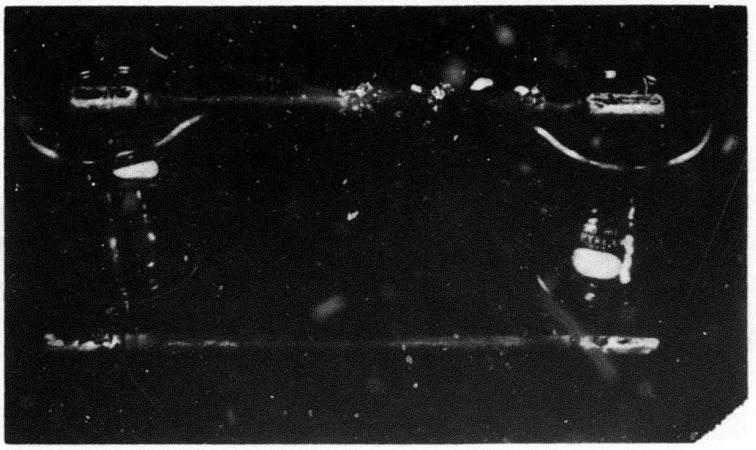

Fig. 8 Lower rod was run for 1587 cycles between room temperature and a peak surface temperature of 1600°C. The upper rod ran 10 cycles to a peak surface temperature of 1700°C.

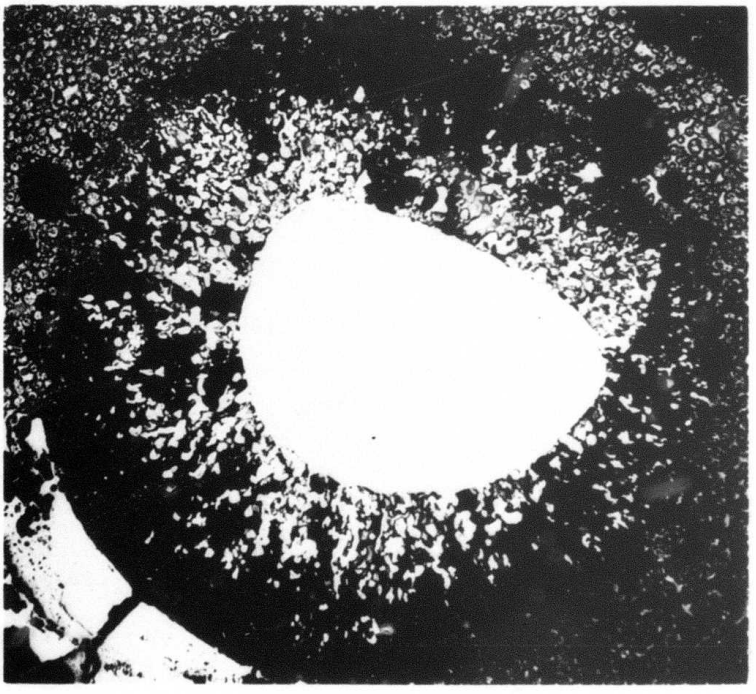

Fig. 9 Cross section of the bubbly portion of rod. 20X

V RESISTIVITY AND THERMAL EMF OF DENSE, DOPED, SINTERED SiC

A. Resistivity

The high temperature stability of 98+% dense, sintered β-SiC coupled with the known electrical properties of single crystals leads to an anticipation that sintered β-SiC might find some unique applications in electrical components. In order to assess this possibility, basic information on electrical properties of sintered β-SiC is needed. The objective of this investigation was to determine whether the electrical conductivity of sintered β-SiC would be affected by dopants in a manner similar to that of β-SiC single crystals. Uncertainty about this arises from the fact that sintered β-SiC always contains boron, which is a necessary sintering additive, at a level (up to 0.4 wt%) which might totally dominate the electrical behavior.

The semiconductive nature of β-SiC has been extensively studied on single crystals, and is described in works by Busch[10], Lely and Kröger[11], Van Daal, et al.[12], Bathe and Hardy[13], and the review by Neuberger[14]. Briefly, atoms of the fifth group (nitrogen and phosphorous) introduce donor levels 0.06 to 0.08 eV below the conduction band which are excited at low temperature and produce conductivity (10^3 - 10^0 ohm^{-1} cm^{-1} at RT). Trivalent atoms (B and Al) form acceptor levels about 0.28 to 0.35 eV above the valence band which are little excited at room temperature. Thus, B and Al doping results in much lower conductivity (10^{-2} - 10^{-5} ohm^{-1} cm^{-1}). In reality, this simple model is rarely applicable because complicating effects arise from other levels almost always present, but whose origin has not yet been identified, from interaction of donors and acceptors, from exhaustion of some donor or acceptors at higher temperature, from degeneracy at high concentrations of dopants, etc.

Previous work done with boron doped hot pressed β-SiC[9] has shown that the effect of boron (as an acceptor forming dopant) can indeed be compensated by nitrogen if a sufficient amount of it has been introduced in the form of silicon nitride. A Si_3N_4 addition thus resulted in n-type behavior in hot pressed β-SiC which exhibited room temperature conductivity on the order of 1 to 5 ohm^{-1} cm^{-1}.

Similar results were obtained in the investigation of sintered, boron doped β-SiC when sintering was done in an atmosphere containing nitrogen. However, since nitrogen retards densification[15], the sintering temperature has to be increased in order to achieve full densification. The nitrogen partial pressure was set by controlling argon and nitrogen flow (pure "tank quality" gasses, less than 10 ppm oxygen according to the supplier) through the carbon resistor sintering furnace. The data on the effect of nitrogen in the sintering atmosphere on the room temperature resistivity of boron doped, β-SiC are summarized in Table I, along with data for boron doped β-SiC sintered in argon.

Resistance was measured with an electronic voltmeter at 6 V DC and 150 AC (with identical results) on 12 mm diameter, 6 mm thick pellets with 6 mm diameter aluminum electrodes sputtered on ground faces.

Boron doped β-SiC sintered in absence of nitrogen or at a low pressure of N_2 exhibits substantial variation in resistivity. Values between 10^2 to 10^4 (Table I) were observed. The origin of this variability is not presently known. The observation that sintering in vacuum tends to increase the resistance suggests that it may be related to furnace atmosphere contaminant such as aluminum or oxygen.

The effect of nitrogen is probably first noticeable at a partial pressure of 100 torr. Further increase in P_{N_2} to 650 torr brings about a drop of three orders of magnitude in resistivity and an unexpectedly high nitrogen content in the sintered body (0.41% N_2).

An interesting preliminary result on the effect of other dopants has been obtained from samples of β-SiC doped with beryllium in the form of a Be_2C addition. This dopant increases low temperature conductivity, but does not measurably affect that at high temperature.

Figure 10 shows resistivity vs. 1/T plots for β-SiC that had been boron doped and: 1) hot pressed; 2) sintered; 3) nitrogen doped and hot pressed; 4) beryllium doped and sintered. All measurements were made on 4 × 1.5 × 25 mm bars with sputtered gold electrodes by a four contact technique at 6 V DC. The activation energies calculated for the boron

TABLE I

Effect of Sintering Furnace Atmosphere on the Resistivity of B-doped, Dense, Sintered β-SiC

Starting powder Code	%B addition	Sintering atmosphere & pressure (torr)	Sintering temperature (°C)	N_2% by vac. fusion	Resistivity RT (ohm-cm)	Remark
ES-11	.5	1 Ar	1950	n.d.	1.7×10^2	hot-pressed
146-1989	.36	760 Ar	2080	<0.005	1.2×10^3	
146-2056	.4	0.2 Ar	2080	n.d.	8.0×10^3	acid leached powder
146-1989	.36	50 N_2	2100	n.d.	1.6×10^3	
146-1989	.36	100 N_2	2190	n.d.	3.3×10^2	
146-1989	.36	450 N_2	2280	0.41	0.32	
146-1989	.36	760 N_2	2300	n.d.	0.51	
146-1893	.9	760 N_2	2180	n.d.	0.80	
146-1989	.36	760 Ar	2050	n.d.	4×10	1.0% Be_2C

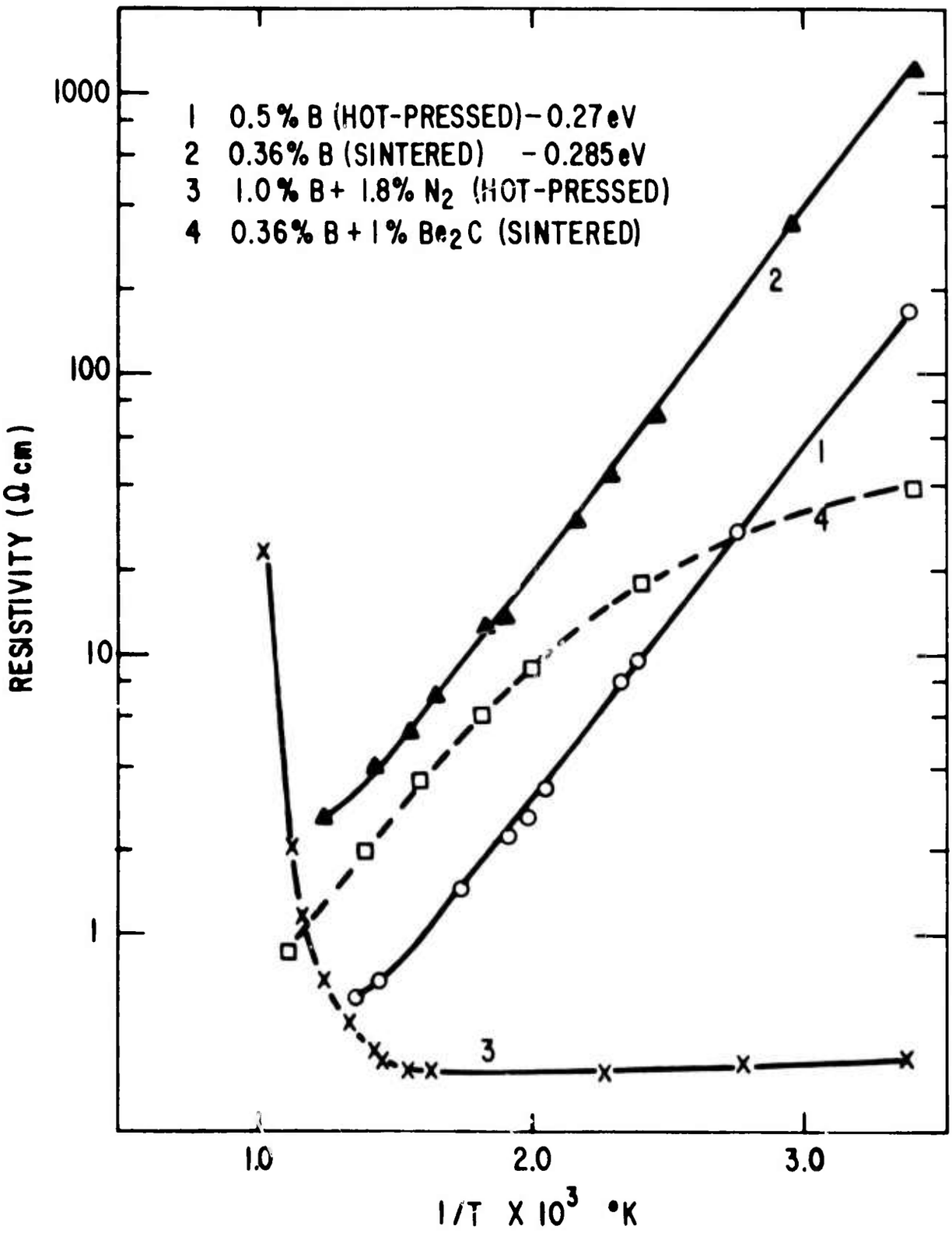

Fig. 10 Resistivity vs 1/T for variously doped, hot pressed and sintered specimens of β-SiC.

doped specimens between room temperature and 600°C were 0.27 and 0.285 eV; values essentially identical to those found for boron doped SiC single crystals[11]. The beryllium/boron doped specimen tends to have a similar activation energy at elevated temperatures. Specimen 3, heavily doped with nitrogen during hot pressing, shows little change in resistance between room temperature and 350°C and a large increase above 350°C. Similar behavior has been reported for nitrogen doped β-SiC single crystals[11]; however, in the present case, the polycrystalline material has a much higher positive temperature coefficient.

B. Thermal EMF

The thermoelectric EMF of a thermocouple made of nitrogen doped β-SiC vs. boron/beryllium doped β-SiC (i.e. of a p-n junction) was measured. For this purpose, circular rods of SiC about 13 cm × 6 mm were isostatically pressed and sintered. The couple was made by "soldering" the sintered rods with silicon into two holes drilled into the side of a short carbon cylinder. The other ends of the rods were copper plated to obtain good contact to wires. The junction was inserted into a platinum wound furnace containing a nitrogen atmosphere and the cold ends were kept at boiling water temperature by inserting them into short, water-filled test tubes. The measurements were taken with an electronic voltmeter with an infinite internal resistance both on heating to 1500°C and on cooling. The resistance of the couple was 480 ohms. Another measurement at low temperature was made with the "cold ends" in an ice bath at 0°C by heating the junction from room temperature to 300°C. The results of both runs are shown in Fig. 11 in terms of EMF vs. temperature difference.

VI INTRODUCTION TO SINTERING INVESTIGATIONS OF COVALENTLY BONDED CERAMICS

The primary task of the work performed under this contract was the investigation of the sintering behavior of covalently bonded solids. Ceramics made of these are in a special class in that they are difficult to fabricate by conventional sintering processes. Until recently, phase-pure

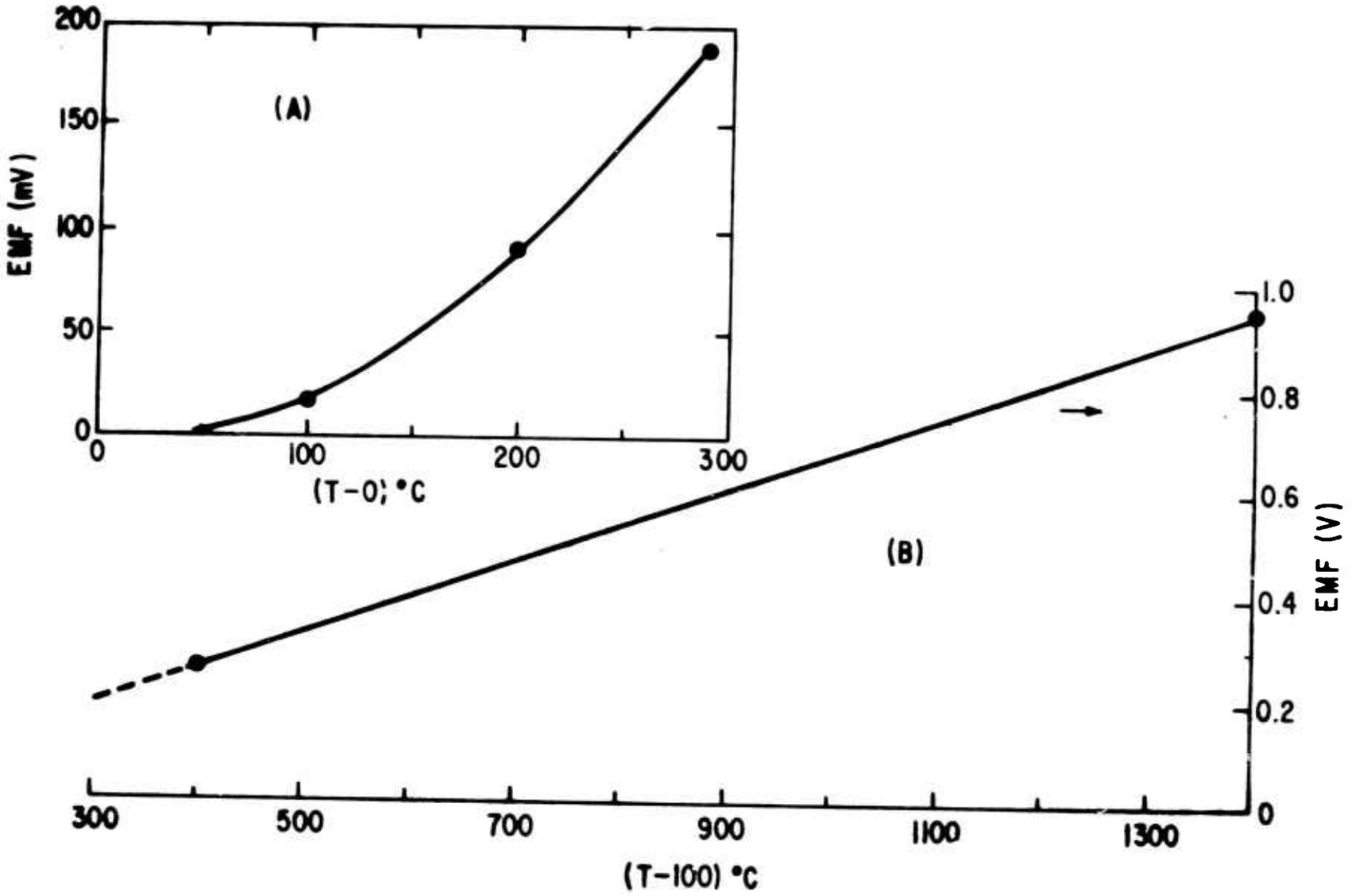

Fig. 11 Thermal EMF of a junction of p- and n-types of β-Sic for: (A) cold junction at 0°C and (B) cold junction at 100°C.

covalent solids such as SiC, Si_3N_4, AlN, and BN could be densified only by the application of high external pressures at high temperatures. The hot pressing of such materials is expensive and limited to fabricating pieces of simple geometry. On the other hand, the densification of powder compacts of several covalent materials (Si_3N_4, AlN) can be achieved by the method of liquid phase sintering in the absence of an externally applied pressure. The presence of a liquid phase on the grain boundaries at high temperature, however, usually has a deleterious effect on high temperature creep and strength, and therefore limits the usefulness of bodies having this type of structure.

Prochazka[9] recently discovered a method of conventionally sintering SiC in the solid state. He added about 0.5 wt% boron and carbon to submicron β-SiC and demonstrated that sintered densities as high as ∿98% of theoretical could be obtained by pressureless sintering. Single phase microstructures (except for some carbon inclusions located in residual pores) could be developed with an average grain size of 2 to 3 microns. It was hypothesized that the boron segregates in the grain boundaries to reduce grain boundary energy while the carbon deoxidizes the surfaces of the β-SiC grains to increase the solid-vapor surface energy, (γ_{GB}/γ_{SV}) is, therefore, decreased so as to allow the occurrence of densification. Prochazka used a geometrical analysis of the interfacial energies and dihedral angles in a porous structure undergoing sintering and came to the conclusion that the requirement for a pore surrounded by three grains to shrink is that the equilibrium dihedral angle (Θ) be greater than 60° or that γ_{GB}/γ_{SV} be $<\sqrt{3}$. The equation which connects these two parameters and applies at the grain boundary-solid vapor interface is

$$\gamma_{GB} = 2\ \gamma_{SV} \cos \frac{\Theta}{2} \quad .$$

The goal of this research program was to develop a better understanding of the sintering of covalently bonded ceramics with emphasis on advances in sintering theory and the generation of dense structures. Special effort was devoted to the determination of sintering mechanisms, whereby doping additions and control of sintering atmosphere enable the conventional sintering of silicon carbide. A study of the development of

interparticle bonds (necks) was undertaken in order to determine the effect of dopants on pore and grain morphology. SiC was chosen for initial study with the hope that understanding the sintering mechanism in this material, for which considerable technology already exists, could be extended to such covalent elements and compounds as Si, Si_3N_4, AlN and BN. Considerable effort was also devoted to the study of sintering of silicon because many of its physiochemical properties are reasonably well understood in terms of defect and impurity effects.

VII SINTERING OF β-SiC

A. Early Stage Sintering of Doped β-SiC

1) Ceramic powders and sintering conditions

The early stage sintering of β-SiC containing carbon only, boron only, and both carbon and boron, was investigated by surface area measurements and scanning electron microscopy. In all cases, the amounts of carbon and boron present was 0.8 and about 0.6 wt%, respectively. The β-SiC powders selected for study were characterized by specific surface areas between 8 and 11 m^2/g. All the SiC powders had about the same concentration of all other impurities. Major impurities were (in ppm) oxygen 1700, tungsten 300, iron 200, chloride 200, nitrogen 80, calcium 50, and aluminum <10.

In some cases the initial sintering of loose powders, as well as that of powder compacts of doped β-SiC, was investigated. Submicron β-SiC powder is generally difficult to die-press without binders, but successful results could be obtained by screening the powder through a -60 mesh nylon screen and die-pressing 3 gram samples in a 5/8" diameter die at 2500 psi. In all cases, the resulting powder compacts were isostatically pressed at 30,000 psi to obtain green densities near 58% of theoretical. (The theoretical density of SiC is about 3.21 g/cc.)

Sintering experiments were performed in flowing Ar (∿5 ppm O_2) at one atmosphere in a carbon element resistance furnace at temperatures between 900 and 2000°C. The effective oxygen pressure inside the furnace was not

determined. Temperature was measured optically and controlled to ±20°C. Investigation of grain growth during sintering of β-SiC containing excess carbon was carried out at 1300°C for times up to about 85 hours. Graphite crucibles were used as containers in every case.

2) Surface area measurements and results

Surface area measurements were made by the single point B.E.T. method* using a continuous flow of 30% nitrogen in helium. By calibrating the system after each nitrogen desorption run, the uncertainty in the specific surface area based on about 5 measurements was reduced to about ±0.2 m^2/g for samples with specific surface areas between approximately 5 and 10 m^2/g. Figure 12 illustrates the effect of sintering temperature on the specific surface area of loose powder and pressed compacts of β-SiC containing carbon and boron. The sintering time at temperature was 10 minutes. For the case of loose powders there is a decrease in the specific surface area with sintering temperature, the initiation of surface area reduction being noticeable at about 1500°C. Pressed compacts, however, exhibit a higher specific surface area than the loose powder up to about 1800°C at which point there is a reversal. It is suggested that the apparent increased area below 1800°C is caused by N_2 condensation in fine capillaries or pores, perhaps 10 to 100 Å in size, that exist in the sintered disks. The difference in specific surface area of the two types of samples sintered above 1800°C is probably caused by the larger number of touching nearest-neighbor grains surrounding a given grain in a pressed compact as compared to that found in a loose powder, thus increasing the number of necks and reducing the solid vapor surface area available for the adsorption or desorption of nitrogen molecules. The specific surface area of sintered, pressed compacts also begins to decrease at about 1500°C with the most rapid reduction occurring between 1800 and 2000°C. It is interesting that shrinkage measurements made on the sintered, pressed compacts (Table II) reveal that the initiation of densification also takes place at

* Surface area analyzer, Quantachrome Corporation, 337 Glen Cove Road, Greenvale, N.Y.

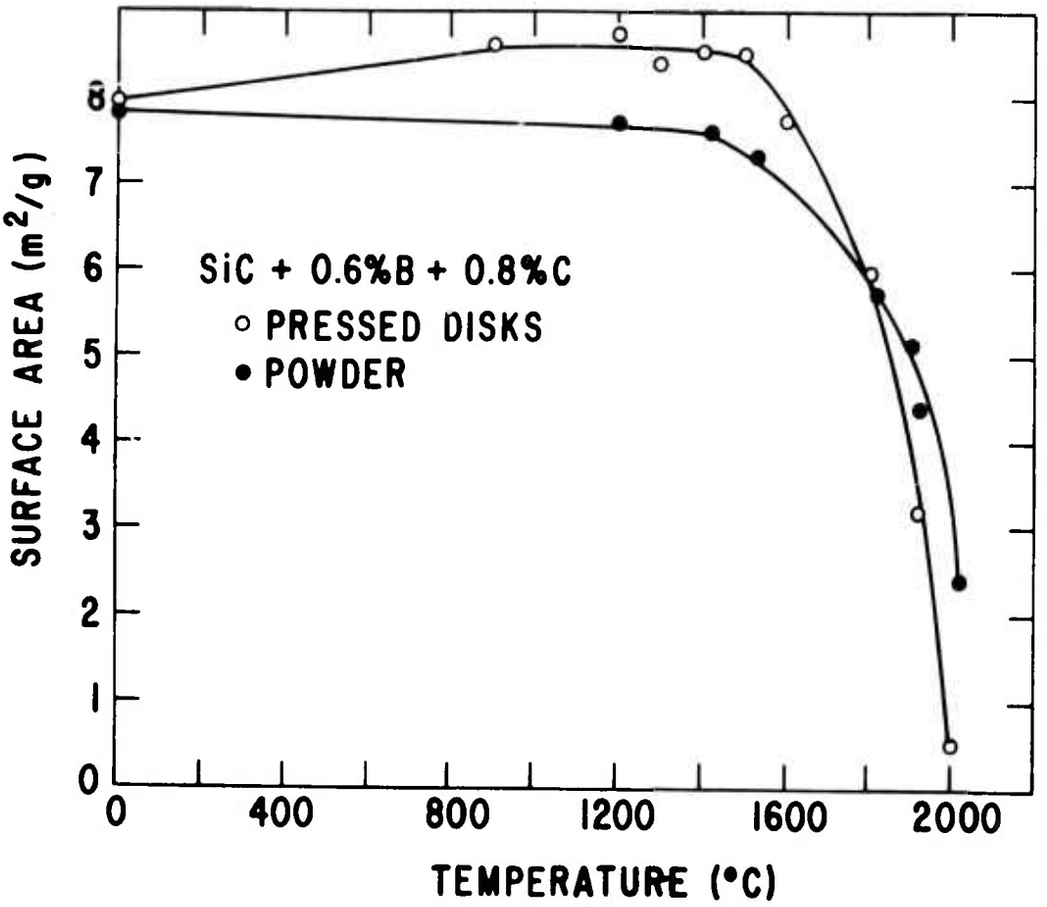

Fig. 12 Specific surface area as a function of sintering temperature for pressed disks and loose powder of β-SiC containing 0.6% B and 0.8% C.

TABLE II

Sintered Densities of Doped β-SiC Compacts
For 1 Hr Hold in Flowing Ar Atmosphere

Composition	D_0/D_t	D_{1500}/D_t	D_{1700}/D_t	D_{1900}/D_t
SiC + 0.8%C	59.2%	59.2%	59.2%	59.2%
SiC + 0.6%B	57.3%	57.3%	58.6%	60.7%
SiC + 0.8%C + 0.6%B	58.6%	59.8%	65.7%	72.3%

D_0 = initial green density

D_t = theoretical density (3.21 g/cc)

D_{1500} = density after sintering at 1500°C

about 1500°C.

β-SiC containing 0.8 wt% carbon responds quite differently to temperature than do those compositions containing both boron and carbon. In Fig. 13 and Table II it can be observed that this material exhibits a decrease in specific surface area at much lower temperatures (near 1250°C) but no densification or shrinkage for temperatures up to 2000°C. The greatest change in specific surface area occurs between 1300 and 1500°C.

The kinetics of surface area reduction in highly porous sintered compacts of β-SiC containing 0.8 wt% carbon can be determined by surface area measurements. Ideally, the approximate relationship between the average size (D) of grains (or particles) with spherical or cubic morphology in a lightly sintered powder compact, and the corresponding specific surface area (S) is

$$D = \frac{6}{\rho S} \quad ,$$

where ρ is the density of the solid in g/cm^2 and D is in microns for S measured in m^2/g. A linear fit of the specific surface area data with sintering time at 1300°C (see Fig. 14) was obtained by plotting $(1/S)^4$ versus time at temperature. Since D is proportional to 1/S, this means that the grain or particle size increases according to $t^{\frac{1}{4}}$. The significance of this relationship will be discussed later.

3) Observation of sintered structures by SEM

Scanning electron micrographs of fired, loose powders and of fractured surfaces of fired, pressed compacts show some interesting structural features depending on the dopant(s) added to β-SiC. The general observations described below are independent of temperature between 1500 and 1900°C except that the differences between the various composition are accentuated at higher temperatures. The SEM photomicrographs of aggregates formed during the firing of loose powders of β-SiC + 0.8% C + 0.6% B shown in Fig. 15 demonstrate that dense, spherically shaped aggregates form in β-SiC containing both carbon and boron (a material that densifies at 1900°C), but β-SiC having only excess carbon (a material which exhibits no densification at 1900°C) consists of an ill-defined aggregated structure

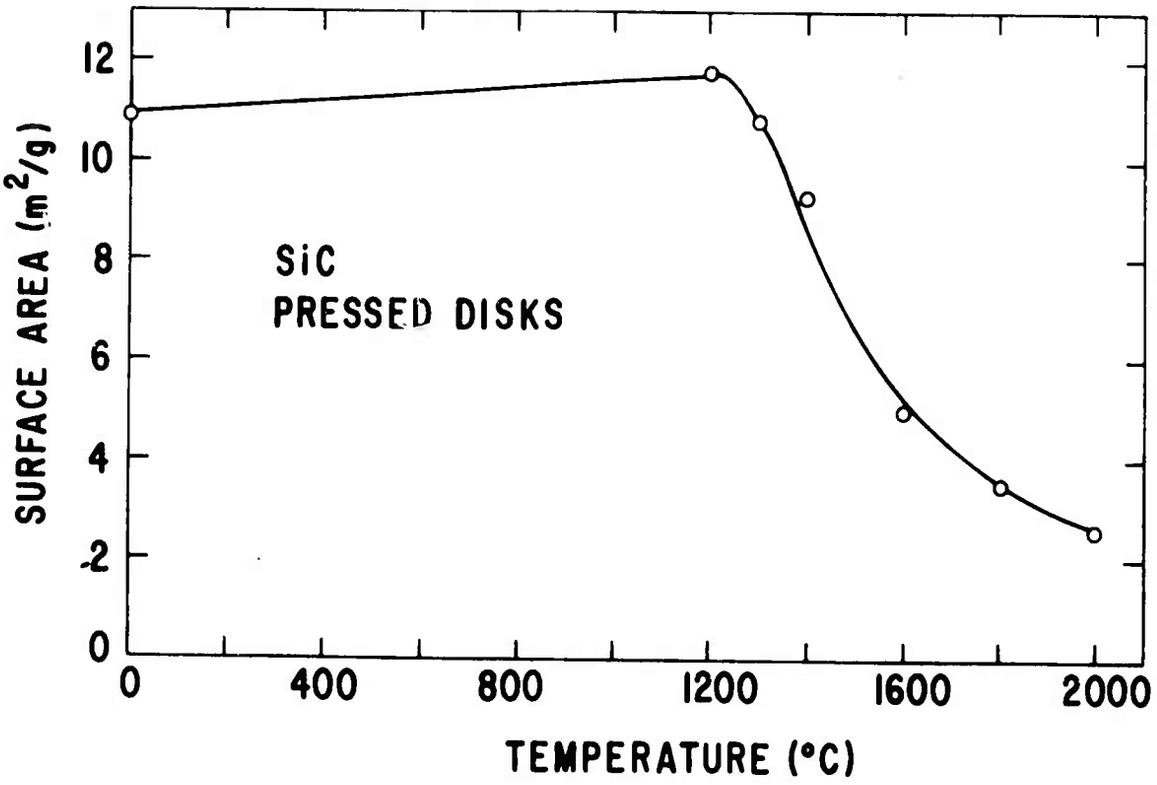

Fig. 13 Specific surface area versus sintering temperature for pressed disks of β-SiC containing 0.8% C.

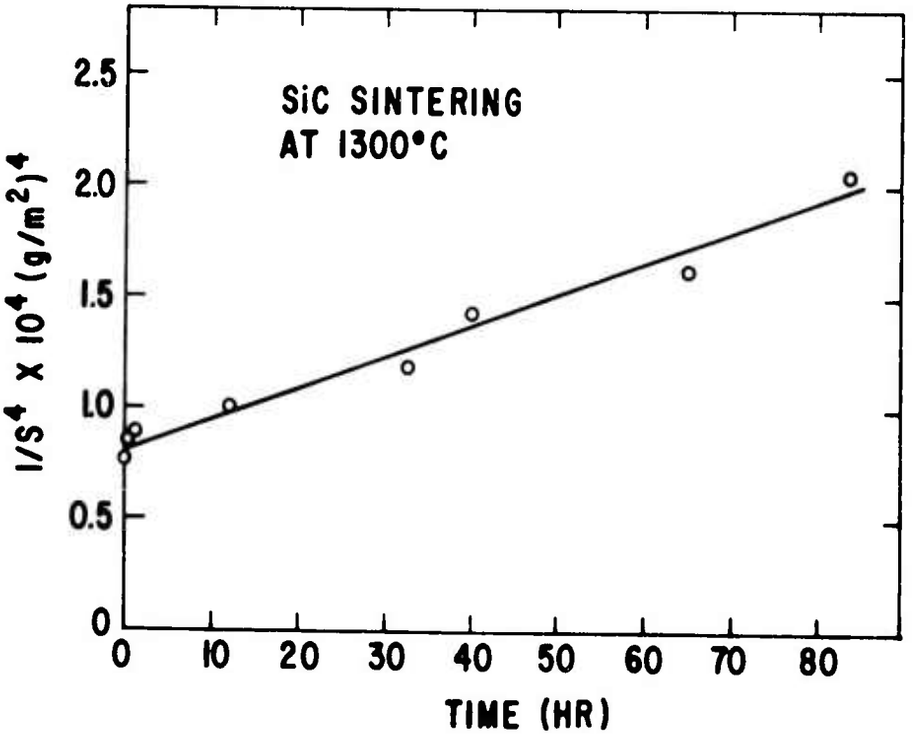

Fig. 14 The kinetics of surface area reduction of sintered, pressed disks of β-SiC containing 0.8% wt%C. Temperature = 1300°C.

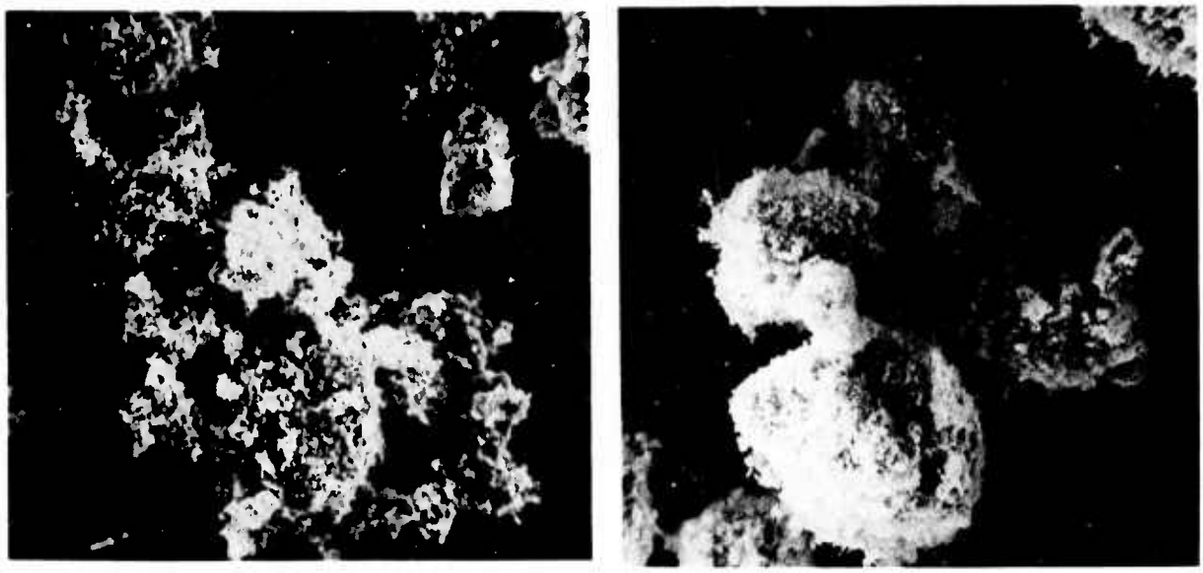

(A) (B)

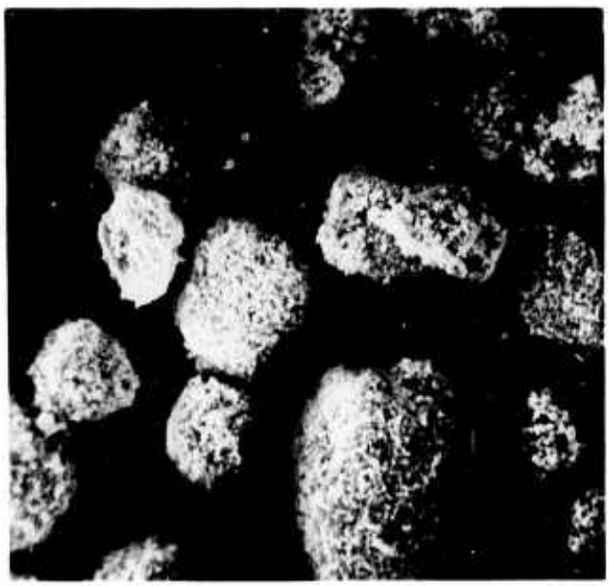

(C)

Fig. 15 SEM photomicrographs of aggregates formed during the sintering of loose powder of β-Sic containing (A) 0.8% C, (B) 0.6% B, and (C) 0.8% C and 0.6% B. The samples were sintered at 1900°C for 1 hr. 480X

which does not "ball-up" upon heating. Fired aggregates of β-SiC doped with boron only exhibit a combination of the structural features of the other two powders. Table II shows that this type of powder is characterized by a small amount of linear shrinkage (about 2%) at 1900°C; the same holds true even at higher temperatures.

SEM photomicrographs, shown in Fig. 16 and 17, were taken from fractured surfaces of lightly sintered compacts. These show some striking differences in the size, shape and appearance of grains and pores as a function of composition. β-SiC containing excess carbon is characterized by a highly porous, interconnected structure having randomly distributed solid regions composed of clusters of grains. The average width of pore spaces between the dense clusters of grains is about 0.8 μ. This is slightly larger than the average grain size which is about 0.6 μ. The dense clusters of grains have an average size of approximately 2.5 μ and are, therefore, much larger than the aberage grain size and pore width.

In contrast, fired compacts of β-SiC doped with boron and carbon have a fine grain and fine pore structure. The grains appear to be equiaxed and have an average size of about 0.3 μ. The average pore size is smaller than the average grain size. Compacts of this composition have densified from about 59 to 72% of theoretical density by firing for 1 hr at 1900°C in flowing Ar.

SEM micrographs of fired compacts of β-SiC having only boron as the dopant reveal a new structural feature, namely, that the grain boundary solid-vapor junctions appear to be more sharply defined. The grains are equiaxed and have an average size of about 0.4 μ. Pore structure can be seen, with the average pore size being about the same as the average grain size.

4) Discussion

Surface area and shrinkage measurements as well as direct observation by scanning electron microscopy can provide considerable information about the development of structure in porous solids undergoing sintering. For example, the early stage sintering behavior of β-SiC doped

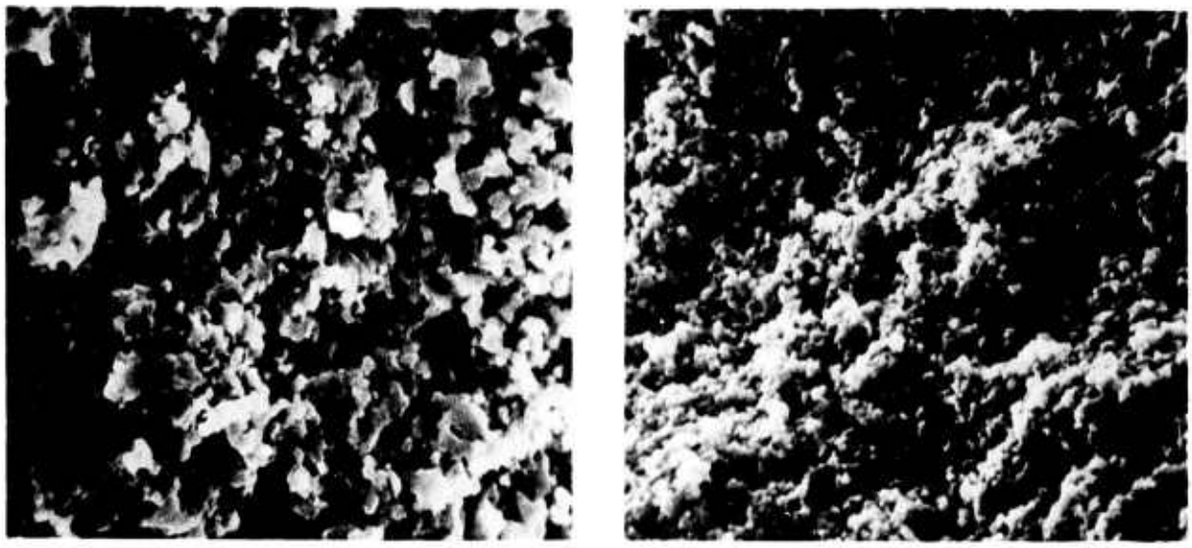

(A) (B)

(C)

Fig. 16 SEM photomicrographs of fractured surfaces of sintered, pressed disks of β-SiC containing (A) 0.8% C, (B) 0.6% B, and (C) 0.8% C and 0.6% B. The specimens were sintered at 1900°C for 1 hr. 1920X

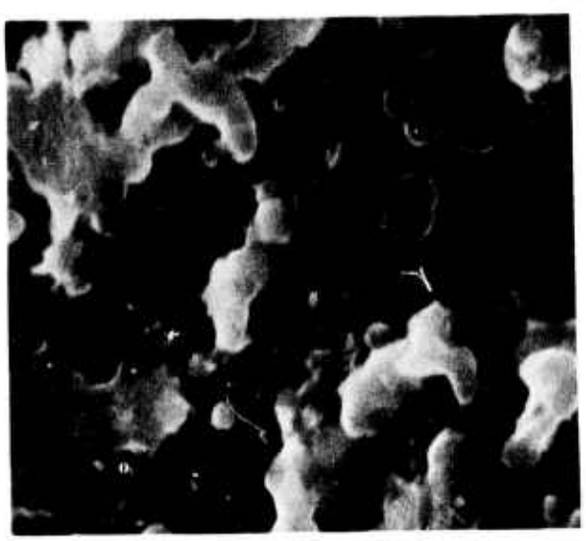

(A)

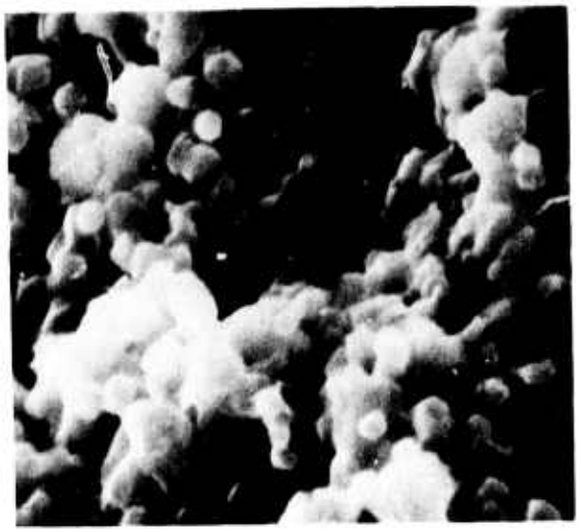

(B)

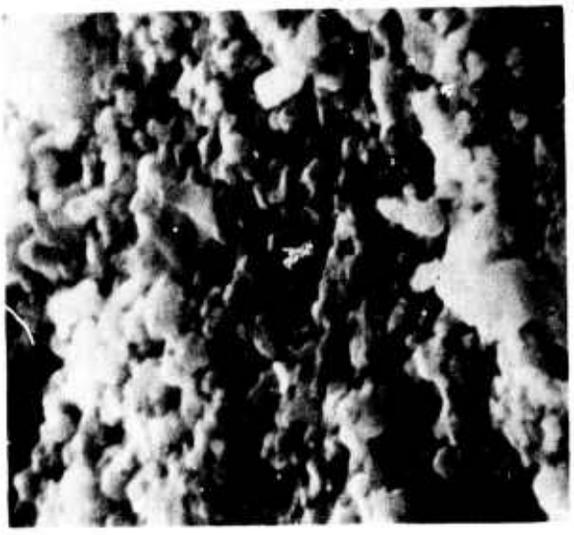

(C)

Fig. 17 SEM photomicrographs of fractured surfaces of sintered, pressed disks of β-SiC containing (A) 0.8% C, (B) 0.6% B, and (C) 0.8% C and 0.6% B. The specimens were sintered at 1900°C for 1 hr. 9600X

with carbon and boron shows that specific surface area reduction and the initiation of densification take place almost simultaneously at 1500°C in a submicron powder. This is a very unusual finding in that most submicron powders of ionic (oxide) materials generally coarsen by surface diffusion at temperatures well below the temperature at which densification begins. The fact that β-SiC powder containing carbon exhibits a decrease in surface area at a temperature near 1250°C and no densification up to 2000°C indicates that the addition of boron to β-SiC containing excess carbon impedes surface diffusion and inhibits grain growth at temperatures up to 1500°C, but permits densification at higher temperatures. The presence of boron and carbon in β-SiC enables the generation of an equiaxed fine-grain structure with a uniform dispersion of small pores. The addition of boron to pure β-SiC gives rise to sintered material characterized by a relatively small grain size (i.e. grain growth by surface diffusion is still minimized) but only a few percent of linear shrinkage takes place. Furthermore, the grain boundary-solid-vapor junctions are clearly evident which indicates that the material is approaching geometrical equilibrium.

The kinetics of grain growth, as deduced from specific surface area reduction, shown in Fig. 14, strongly indicate that the mechanism is one of surface diffusion. Greskovich and Lay[16] showed that grain growth or particle coarsening in porous compacts may be viewed as the growth of the neck regions between two particles followed by the rapid migration of the grain boundary developed between the particles through the smaller of the two. They used Nichols and Mullins[17] equations for the time required to fill a neck between two spheres of arbitrary size by surface diffusion and arrived at the conclusion that surface diffusion-controlled grain growth in very porous compacts should approximately follow a $t^{\frac{1}{4}}$ dependence. Our experimental data agree well with this prediction.

B. Grain Growth and Densification in β-SiC Containing Boron and Carbon

In an attempt to further understand the factors controlling the sintering of covalently bonded β-SiC, an investigation of grain growth and densification was undertaken at high temperatures. These two processes are

found to be interrelated during sintering of ionic and metallic powders, such as Al_2O_3 and Cu, respectively, in a manner such that the activation energy is nearly the same for grain growth and densification. In the case of Cu, the experimentally observed activation energy for densification is about 46 Kcal/mole[18] and agrees well with the activation energy for volume self-diffusion[19]. An investigation of the atomic mobility in β-SiC doped with B and C was pursued through grain growth experiments.

Two types of β-SiC powders, containing both C and B, were investigated. These powders are designated as Powder I and Powder II, and are characterized in Table III. Early in the sintering of Powder II, large tabular grains formed in the porous compacts and made it impossible to calculate a realistic value for the activation energy for grain growth. The sintering behavior of Powder II will, therefore, be discussed in the last part of this section.

1) Sintering behavior of Powder I

Disk-shaped powder compacts were formed by die-pressing 3 g samples in a 5/8" diameter die at 2500 psi followed by isostatic pressing at 30,000 psi to obtain green densities of about 59% of theoretical (the theoretical density of β-SiC is about 3.21 g/cc).

Sintering experiments were performed in flowing Ar (∿5 ppm O_2) at one atmosphere in a carbon element resistance furnace. Specimens were fired in a graphite crucible for 1 hr hold times at various temperatures from 1500°C to 2100°C. The effective oxygen pressure inside the furnace was not determined. Temperature was measured optically and controlled to ±20°C. The apparent density of a sintered piece was calculated from its mass and volume. Grain size was determined from scanning electron micrographs of fractured surfaces at magnifications of 10,000X by measuring approximately 50 to 100 grains in each specimen.

The results of the grain size and density measurements of the sintered specimens are given in Fig. 18 as a function of sintering temperature. Approximate error bars are shown on representative data points. The shapes of these curves are similar to those found for the sintering of Al_2O_3 and

TABLE III

Characterization of β-SiC Powders I and II

	POWDER I	POWDER II
Method of preparation	gas phase reaction in plasma torch	solid state reaction Si+C
Composition	β-SiC+0.8 wt% C+0.6% B	β-SiC+0.7 wt% C+1% B_4C
Specific surface area	8 m^2/g	11 m^2/g
Major impurities (ppm)	O 1700, W 300, Fe 200, Cl 200	O 4400, Fe 270, Al 150
Phase purity	>98% β-SiC	>98% β-SiC

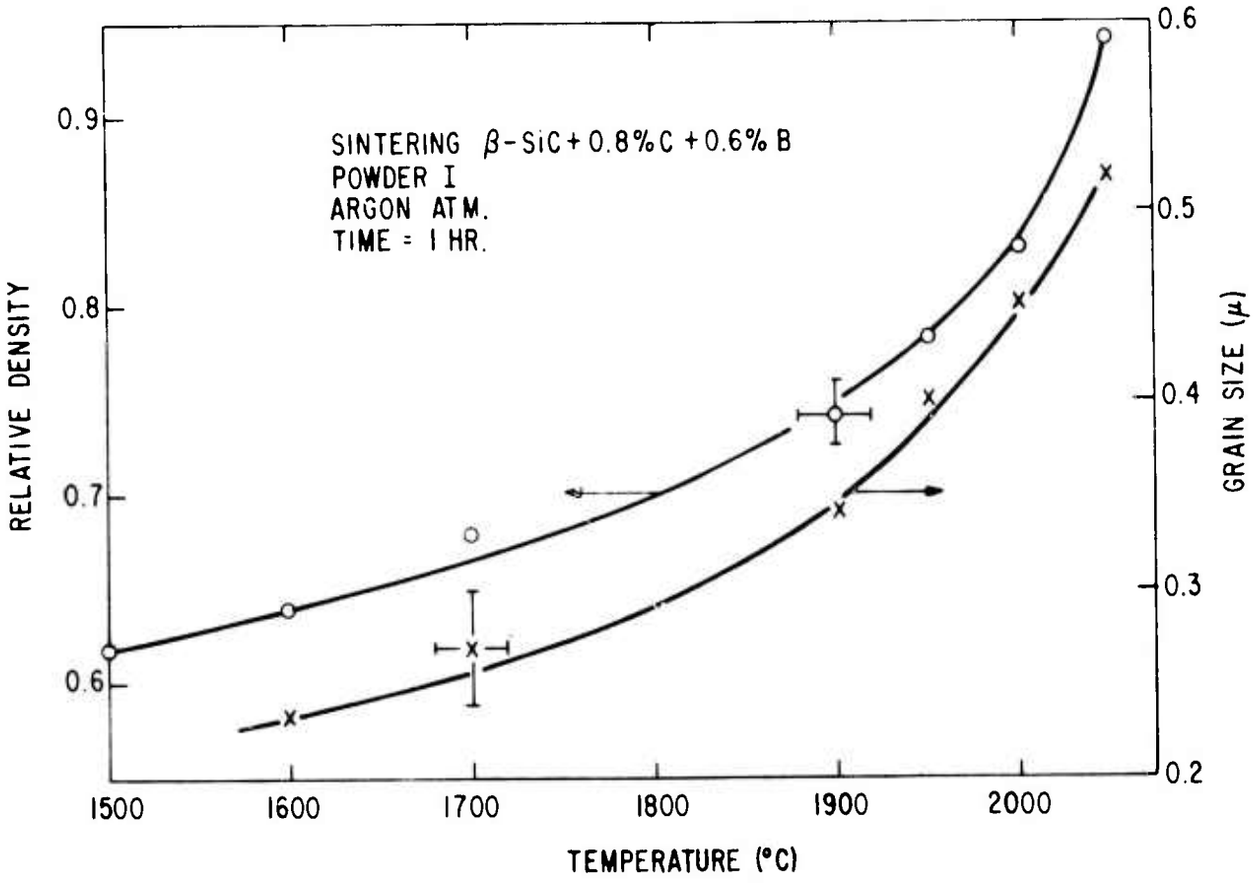

Fig. 18 Relative density and grain size as a function of sintering temperature for Powder I.

other ionic materials. If it is assumed that a cubic grain growth law is obeyed, as is found during the sintering of most ionic materials, then an activation energy for grain growth can be calculated. Hence it is assumed that

$$d^3 - d_o^3 = k(t - t_o) \qquad (1)$$

where d is the average grain size, d_o is the initial average grain or particle size, k is the temperature-dependent grain growth rate constant, t is time at temperature and t_o is the induction time for the beginning of grain growth. It is assumed that $t >> t_o$. The grain growth rate constant is calculated at each temperature according to Eq. 1. By using the defining equation for k,

$$k = k_o \exp(-Q/RT) \qquad (2)$$

where k_o is a constant, Q is the activation energy for grain growth and RT is thermal energy, the slope of the plot of log k vs. 1/T is equal to -Q/2.3R. Such a plot on semilogarithmic coordinates is shown in Fig. 19. The activation energy was calculated to be approximately 80 Kcal/mol. This magnitude of activation energy for grain growth in covalently bonded β-SiC containing 0.8 wt% C + 0.6% B is not unusual when compared to values obtained for oxides. In fact, this activation energy is lower than expected and is lower than those (150 Kcal/mol and 104 Kcal/mol, respectively) found for grain growth in Al_2O_3[20] and BeO[21].

The kinetics of microstructural development at 2000°C was followed by SEM photomicrographs (Fig. 20) of fractured surfaces of the sintered specimens and by measuring density versus time (Fig. 21). It was hoped that grain growth kinetics could also be obtained from such photomicrographs. However, due to the small changes in grain size occurring with time at temperature, no reliable data could be obtained. A further complicating factor in determining the grain growth kinetics was the formation of large, dense, solid regions in the fine-grained matrix. This microstructure development is clearly shown in Fig. 20. A polished section of a sample sintered for 300 min at 2000°C is shown in Fig. 22. There is a large size distribution of "blocky" dense, solid regions which range from

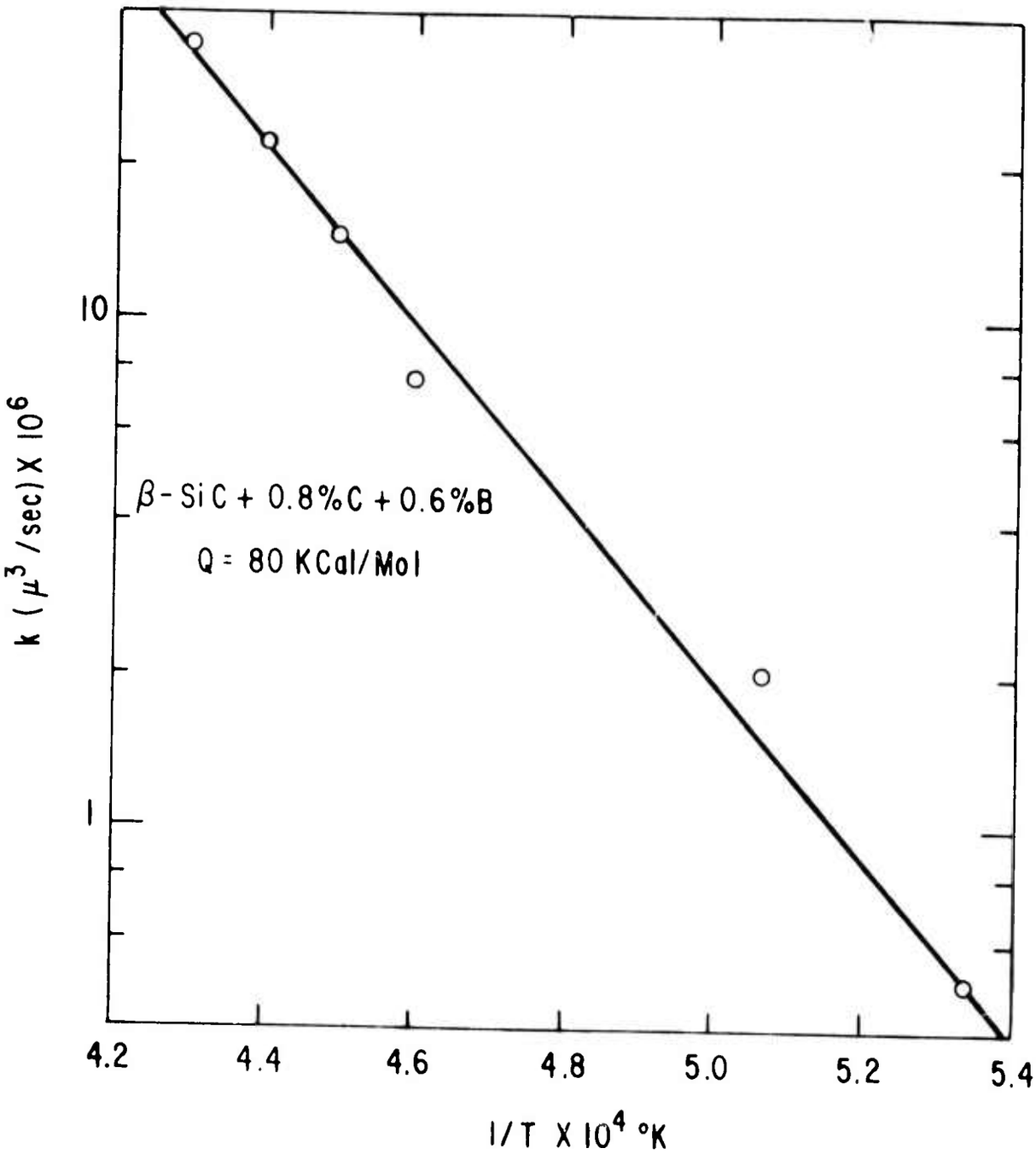

Fig. 19 Cubic grain growth rate constant versus reciprocal temperature for Powder I.

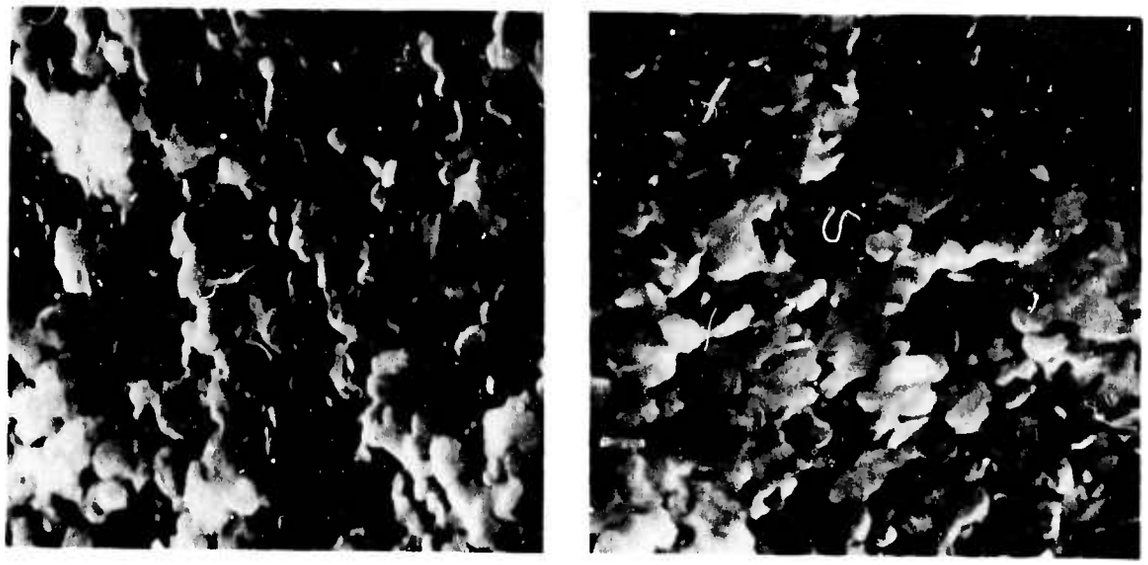

A B

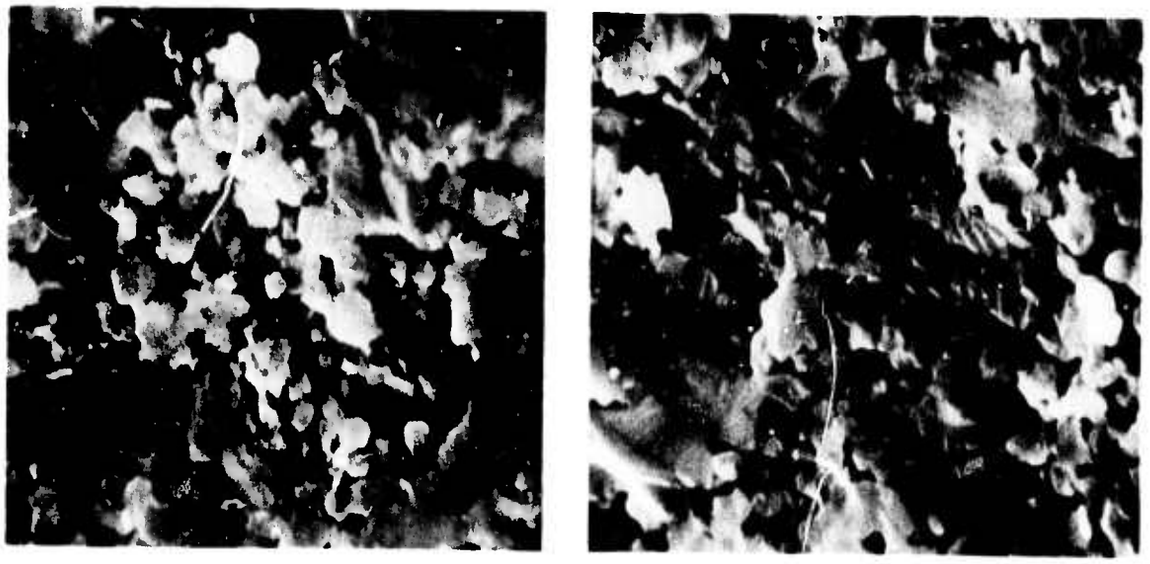

C D

Fig. 20 SEM photomicrographs of fractured surfaces of sintered specimens of Powder I (β-SiC + 0.8% C + 0.6% B) heat treated at 2000°C for (A) 2 min, (B) 10 min, (C) 60 min, and (D) 300 min.
10,000X

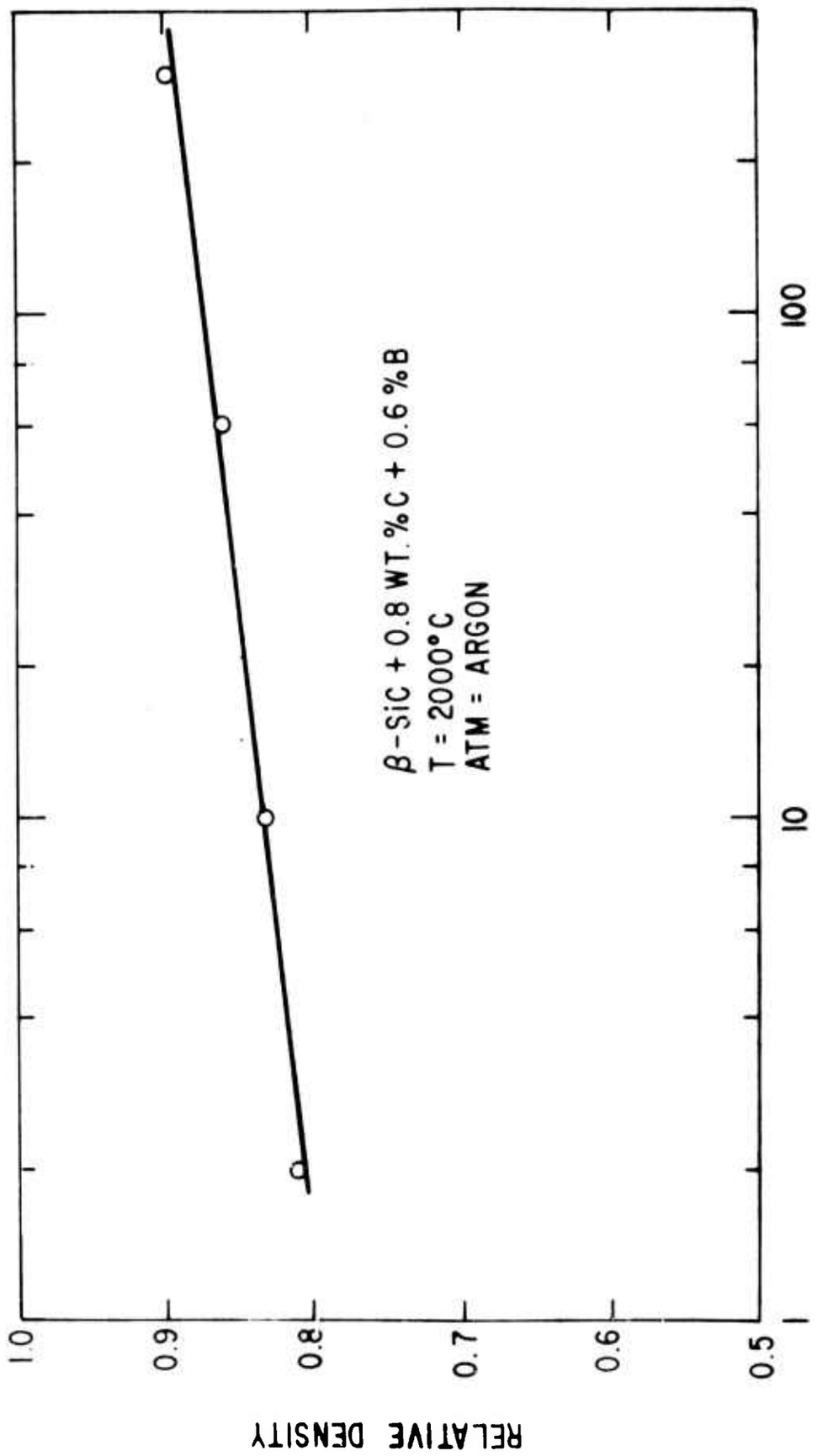

Fig. 21 Relative density versus logarithm of time for Powder I (β-SiC + 0.8 wt% C + 0.6% B) sintered at 2000°C in argon.

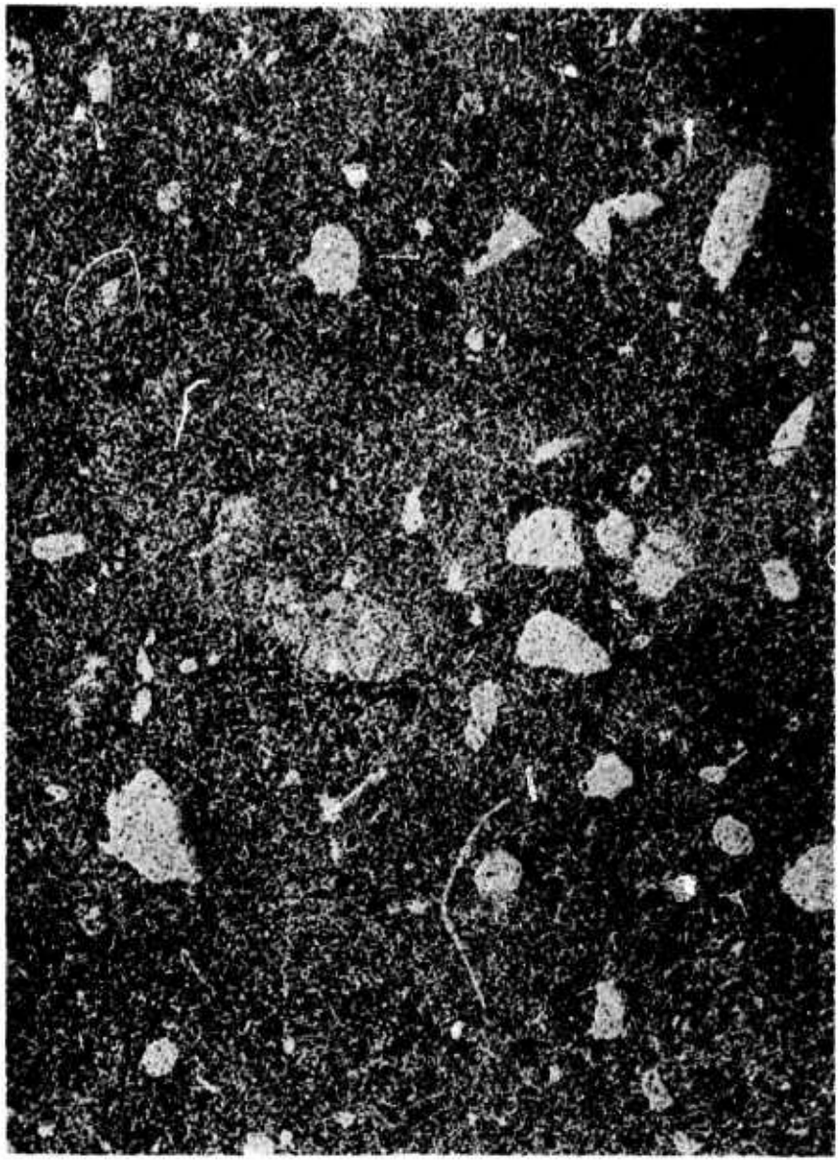

Fig. 22 Polished section of a specimen of Powder I (β-SiC + 0.8% C + 0.6% B) sintered for 300 min at 2000°C. Note large dense regions in the microstructure. 150X

about 1 to 100 μ in the fine-grain (∿0.5 μ) β-SiC matrix. A chemically etched, polished section reveals that these dense regions are polycrystalline (Fig. 23). The origin of these regions is believed to be associated with the size distribution of aggregates known to exist in this unprocessed, β-SiC powder. This speculation is supported by the fact that such "blocky", dense regions do not form during the sintering of the same powder if it receives a ball milling treatment to comminute the particle aggregates. In order to fabricate sintered β-SiC articles having high strength, it is mandatory that the powder be processed to insure the development of a homogeneous, fine-grained microstructure.

Figure 21 illustrates the linear relation between relative density and the logarithm of sintering time. This relationship is frequently found in the sintering of oxides and metals, and according to recent work[18], can be understood on a theoretical basis if grain growth kinetics follow a cubic law. It, therefore, appears that the isothermal densification kinetics for covalently bonded β-SiC, doped with B and C, are not atypical.

2) Sintering behavior of Powder II

The characterization of Powder II is shown in Table III. This β-SiC powder was synthesized from the elements by a solid state reaction, $Si + C \rightarrow SiC$, and subsequently leached with $HF + HNO_3$ to remove free Si, and then heated at <600°C in air to burn off free C. The specific surface area of the starting powder is not much different from that of Powder I. Addition of 0.5 to 0.8 wt% boron in the elemental form or as B_4C has been found to have the same effect on the sintering of Powder I[22]. Hence, the different sources of the boron in these two powders should not affect the sintering behavior. Finally, Powder I has only about 40% as much oxygen impurity as that found in Powder II.

The relative density and specific surface area of sintered compacts of Powder II are listed in Table IV and compared with those measured for Powder I. It is interesting that compacts of Powder II exhibit ∿17% reduction in specific surface area after firing at 1700°C for 1 hr, but no densification. Compacts of Powder I, on the other hand, densify about 9%

Fig. 23 Microstructure of a dense, solid region in sintered β-SiC containing 0.8% C and 0.6% B chemically etched in 10 parts KOH + 1 part KNO_3 at 650°C for 30 seconds.

1000X

TABLE IV

Comparison of Relative Density (D) and Specific Surface Area (S.A.) of Sintered Compacts of Powders I and II

	POWDER I		POWDER II	
Sintering conditions	D(%)	S.A. (m^2/g)	D(%)	S.A. (m^2/g)
As pressed	59	8	53	11
1500-1 hr-Ar	60	8.5	53	11
1600 1 hr-Ar	64	7.8		
1700-1 hr-Ar	68	6	53	9.1
1900-1 hr-Ar	74	4	65	3.4
2100-1 hr-Ar	96		86	

at 1700°C while the surface area reduces to about 25% of its original value. Densification of Powder II begins somewhere between 1700 and 1900°C and reaches a maximum value of 86% of theoretical at 2100°C. Prolonged sintering times and/or higher temperatures do not increase the density beyond 86%. By comparison, sintered samples of Powder I can be made with densities as high as 96% of theoretical by firing at 2100°C.

A question to be answered is why do sintered specimens of Powder II have a limiting density near 86%. The answer may possibly be found in SEM photomicrographs of fractured surfaces of specimens sintered at 1700, 1900 and 2100°C in argon for 1 hr (Fig. 24). The microstructure of the specimen sintered for 1 hr at 1700 C shows a very fine grain and pore structure. After 1 hr of sintering at 1900°C, long thin plates have already developed in the fine-grained matrix of the sintered specimen which is only 66% dense. Dense plates as long as 20 μ and approximately 0.6 to 0.8 μ thick are visible in Fig. 24B. By increasing the sintering temperature to 2100°C (Fig. 24C), there is an increase in the length and number density of these dense plates. Furthermore, the average pore size appears to increase with increasing temperature (compare Figs. 24B and 24C). X-ray diffraction analysis has identified the plates as α-SiC.

It is believed that the low final density of Powder II (∿86% of theoretical) is associated with the formation of large α-SiC plates growing in the fine-grained β-SiC matrix. The large α-SiC plates can reduce the shrinkage rate of the much finer (0.3 μ) β-SiC grains by a particle-size dilution effect. This type of effect is expected from sintering theory. A more important effect which strongly retards densification is the development of a continuous network of α-SiC plates which acts to rigidize the sintering body (see Fig. 24C). Once the large α-SiC plates impinge on one another to make a continuous framework throughout the structure, densification essentially ceases because the coordinated atomic adjustments at the grain boundaries necessary to accommodate shrinkage cannot occur. Finally, it may be speculated that the higher content of oxygen or other impurities in Powder II helps to promote the phase transformation from β → α-SiC.

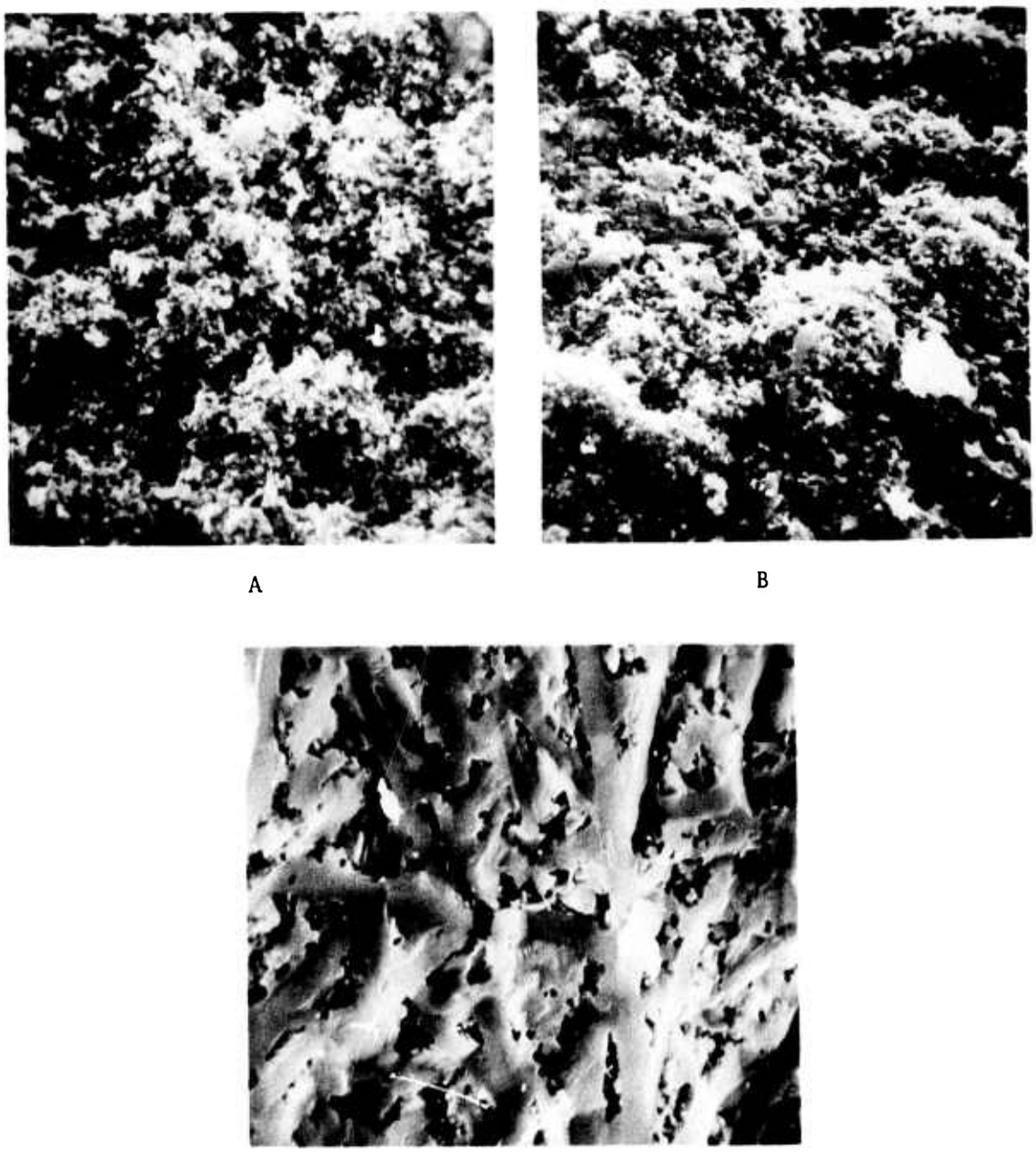

Fig. 24 SEM photographs of fractured surfaces of specimens of Powder II (β-SiC + 0.7% C + 1% B_4C) sintered for 1 hr in argon at (A) 1700°C, (B) 1900°C and (C) 2100°C. Note long plates of α-SiC in (B) and (C). 2000X

C. Dihedral Angles in Sintered β-SiC

On the basis of thermodynamic considerations it has been hypothesized[9] that densification can only take place in a sintering solid if the equilibrium dihedral angle (Θ) is greater than 60° for a pore surrounded by 3 grains; or that γ_{GB}/γ_{SV}, the ratio of the grain boundary to solid-vapor surface energy, be $<\sqrt{3}$. These parameters are interrelated by Young's equation -

$$\gamma_{GB} = 2\gamma_{SV} \cos \frac{\Theta}{2} \quad . \tag{3}$$

Transmission electron and scanning electron microscopy were employed to observe dihedral angles in β-SiC containing carbon, boron and carbon, and only boron. Three sample preparation techniques were used to help reveal grain boundary-solid vapor intersections in these materials. In the case of TEM studies, 1) sintered powders were ultrasonically dispersed, placed on carbon substrates and then photographed by electron transmission or 2) sintered samples were thinned in an ion micromilling apparatus and then examined by direct electron transmission. SEM was used to observe fractured surfaces of sintered compacts.

A large number of dihedral angles were observed in the photographs shown in Fig. 25-30. Photomicrographs of sintered particles of β-SiC + 0.8% C shown in Figs. 25 and 26 reveal that all dihedral angles observed appear to be larger than 100°. A pore surrounded by 5 grains in a sintered compact of this material is shown in Fig. 27. Again, the dihedral angles appear to have values near 100°. Figure 28 is a SEM photomicrograph of the same powder which was first hot pressed to 79% of theoretical density at 2050°C at 10,000 psi for 1 hr and then sintered at 1900°C for 2 hrs without any further change in density. Note that nearly all dihedral angles are well over 100°. Because these dihedral angles are much higher than the critical angle of ∿60°, this powder should have no thermodynamic limitations on densifying during sintering. However, it is observed experimentally that compacts of this powder will not shrink to any extent even when heated to temperatures ∿2100°C.

Boron doped β-SiC powder (S.A. ∿8-10 m^2/g), likewise, does not densify

Fig. 25 TEM photomicrograph of sintered particles of loose powder of β-SiC containing 0.8% C fired at 1900°C for 1 hr in argon. 24,400X

Fig. 26 TEM photograph of a group of sintered particles of β-SiC. Sintered at 1900°C for 1 hr in argon. 55,000X

Fig. 27 Five-sided pore in the microstructure of a powder compact of β-SiC containing 0.8% C that was sintered at 1900°C for 1 hr in argon. 97,500X

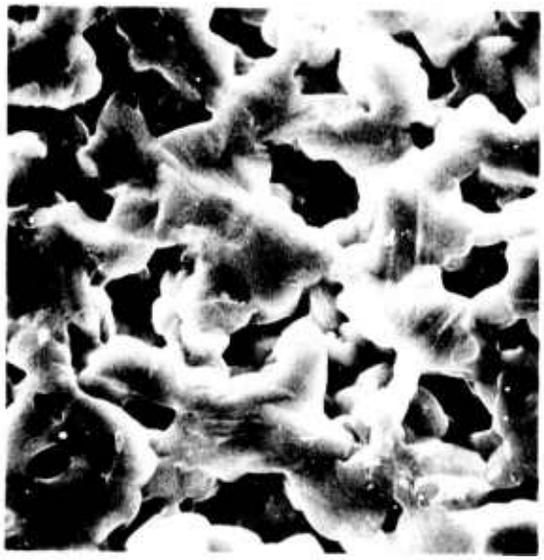

Fig. 28 Microstructure of hot-pressed β-SiC containing 0.8% C which was subsequently annealed at 1900°C for 2 hrs in argon. 1840X

Fig. 29 Sintered particles of loose powder of β-SiC containing 0.6% B fired at 1900°C for 2 hrs in argon. 64,000X

Fig. 30 Sintered particles of loose powder of β-SiC containing 0.8% C and 0.6% B fired at 1900°C for 2 hrs in argon. 57,000X

more than 1% even at very high temperatures. Inspection of the neck regions between sintered particles shows that the dihedral angles are also more than 100° (see Fig. 29). Similar large dihedral angles are observed in highly sinterable powders, such as Powder I, which contain both C and B additions. Such a powder is shown in Fig. 30.

Observations of the dihedral angle at the junction of a grain boundary with the solid-vapor surface of a pore show, therefore, that the dihedral angle is larger than 100° in β-SiC powders that do not densify just as in those that do densify during sintering. It may be that grain boundaries of high energy orientation, which would produce small dihedral angles, are so unstable that they may not form at all. This could be the reason why small dihedral angles (<70°) have not been observed in any microstructure developed in the intermediate stage of sintering.

D. Development and Shrinkage of Grain Boundaries in β-SiC Containing 0.8% C

The development of microstructure during the early stage sintering of β-SiC powder containing carbon only was discussed in section VII-A-3. Compacts of this powder do not exhibit densification at temperatures up to 2100°C in Ar. The microstructure of this material when sintered at 1900°C is shown in Fig. 31 along with that of the unsintered or "green" material. Sintered β-SiC containing excess carbon is seen to be characterized by a highly porous, interconnected structure having randomly distributed, highly dense regions composed of clusters of grains. The average grain size is about 0.6 μ and the average size of a cluster of grains is ∿2.5 μ. A cluster contains, on the average, about 72 grains, assuming that the grains are spherically shaped. Put another way, the number of original powder particles, 0.17 μ in average size, required to produce one dense cluster of grains is more than 3,000.

To account for this kind of microstructure, it is postulated that a large number of interparticle contacts either do not develop into grain boundaries or that, once developed, they break; perhaps as a result of local tensile stresses which develop during the early stages of sintering. An

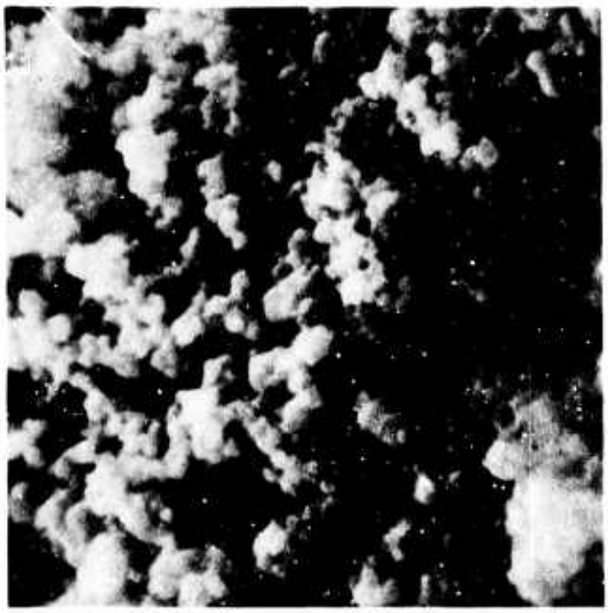

A

B

Fig. 31 SEM photomicrographs of a fractured surface of (A) a "green" compact and (B) sintered compact (1900°C-1 hr-Ar) of β-SiC powder containing 0.8% C.

experiment done to check this idea was to hot press some of this same β-SiC powder containing excess carbon in order to force the formation of a large number of grain boundaries per unit volume. The hot pressed specimen was then annealed without pressure being applied and the changes which occurred in the pore-grain structure observed by SEM.

The photomicrographs in Figs. 32-34 show microstructures of sintered, hot pressed, and hot pressed and annealed β-SiC containing 0.8% C. First of all, as a reference structure, Fig. 32 is the microstructure of a powder compact which has only been sintered at 1900°C for 1 hr. The microstructure of a sample hot pressed at 2050°C for 1 hr at 10,000 psi is shown in Fig. 33. Photomicrographs of the hot pressed sample which was subsequently annealed at 1700°C and 1900°C are shown in Figs. 34A and 34B, respectively. The sintered sample has a relative density of 59%, the same as that of the original green compact. The hot pressed sample densified to a relative density of 79%, but the subsequent annealing treatments caused no further change in density to occur. A comparison of grain sizes in the sintered and hot pressed β-SiC indicates that the hot pressed specimen has about twice the grain size (∿1.2 μ) of the sintered specimen (∿0.6μ). The larger grain size is due to the higher temperature used during hot pressing (2050 vs. 1900°C).

Annealing the hot pressed sample at 1700°C causes little change in microstructure except for some smoothing of solid surfaces, probably by surface diffusion. A major transformation in microstructure occurs during annealing at 1900°C for 2 hrs, since an appreciable amount of grain growth and pore growth occur. The resulting microstructure is identical to that of the sintered sample except for a change in scale. Since a major amount of grain and pore growth occur during the 1900°C anneal, a temperature 150°C below the hot pressing temperature, the microstructure of the hot pressed sample must be very unstable with respect to thermal treatment at 1900°C in the absence of an applied pressure. The instability in structure is believed to originate from the instability of a large number of high energy grain boundaries which are metastable-to-stable during hot pressing when compressive forces are applied, but become unstable in the absence of

Fig. 32 Microstructure of a sintered specimen of β-SiC containing 0.8% C fired at 1900°C for 1 hr in argon. SEM of fractured surface. 2000X

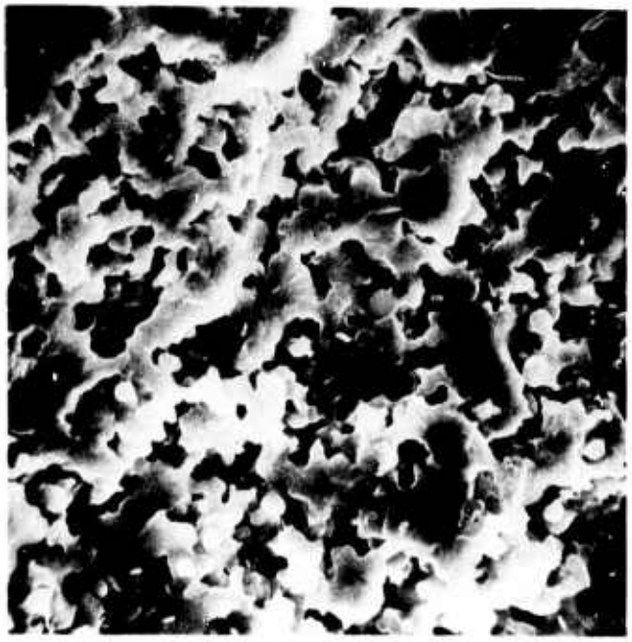

Fig. 33 Microstructure of a hot-pressed specimen of β-SiC powder containing 0.8% C. Specimen was hot-pressed at 10,000 psi for 1 hr at 2050°C. SEM of fractured surface. 2000X

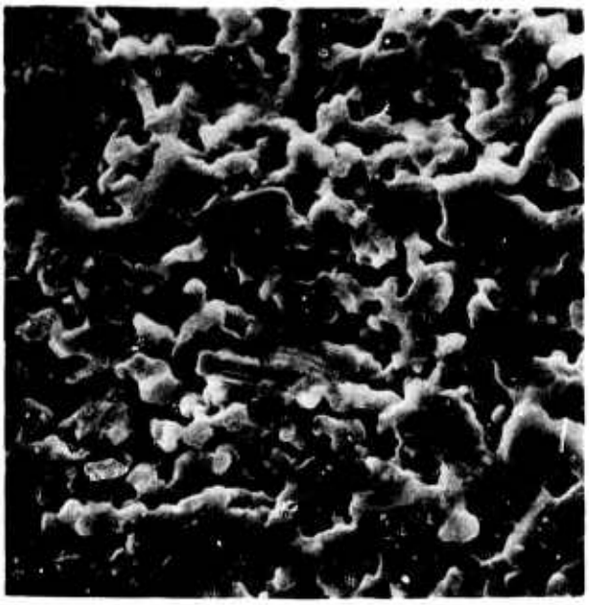

A

B

Fig. 34 Microstructure of hot-pressed β-SiC containing 0.8% C which was (A) annealed at 1700°C and (B) annealed at 1900°C for 2 hrs in argon. SEM of fractured surface. 2000X

such compressive forces. During subsequent sintering at temperatures where sufficient matter transport can occur, these high energy grain boundaries shrink, thus ultimately breaking the contact between grains within a certain range of mutual orientation. This process is accompanied by high surface diffusion which permits rapid grain growth (coarsening) and pore growth in these porous microstructures. In Figs. 34A and 34B, several narrow "necks" or grain boundaries can be seen which may indicate those grain boundaries which are in the process of disappearing.

VIII SINTERING OF SILICON

A. Introduction

Silicon is a covalently bonded solid which is generally regarded as being unsinterable. It is ideal for the study of sintering in covalent solids because it can be obtained in high purity form and a wealth of information has been accumulated on its physical and chemical properties in single crystal form, including impurity diffusion data. Technologically, sintered silicon could be an important source material for the formation of reaction-bonded Si_3N_4. Furthermore, large complex shapes of theoretically dense, polycrystalline silicon may have potential applications in a variety of electronic applications.

The sintering behaviors of silicon powders were investigated to determine the characteristics they have in common with those of β-SiC powders. Similar work on Si_3N_4 and AlN powders is reported in subsequent sections. The studies are aimed at revealing the causes of the normal "unsinterability" of the whole class of powders of covalently bonded solids.

B. Sintering Crystalline Silicon Powders

1) Powder preparation

The silicon used had been purchased from Monsanto Research Corp., St. Peters, Missouri. It is their hyperpure grade prepared by thermal decomposition of trichlorosilane and is used for manufacturing semiconductors. It was obtained in the form of polycrystalline chunks

about 1" in diameter which were broken pieces of a rod pulled from a melt. The minimum resistivity of the silicon was 100 ohm-cm which indicated a total impurity content of less than about 2 ppb. The chunks were crushed with a mortar and pestle of high purity copper. The resulting powder was sieved through brass screens and then leached in aqua regia for 24 hours to dissolve any metal. The acid was changed after the first 4 hrs. After leaching, the powder was washed thoroughly with distilled water and dried.

Fine particles of silicon in the micron-to-submicron size range were prepared by feeding -325 mesh silicon particles into a Trost fluid energy (jet) mill. This type of milling device has the significant advantage of producing fine powder with control of particle size and distribution while maintaining purity. This mill functions by making use of compressed air to carry the particles to be broken. This is expanded through two diametrically opposed jets to achieve high relative velocities of the particles so that fracture by mutual impact can occur. The fractured particles are then passed through a classifier, and the fines collected. The structure of the collection system permitted silicon powders with an average particle size of 1.35 μ and 0.23 μ to be collected in different regions. These average particle sizes were determined from surface area measurements made by the B.E.T. method using flowing 30% N_2 in He.

A typical chemical analysis of a jet milled powder showed that the major impurities were 2000 ppm O, 300 ppm B and 100 ppm of Cu, Fe and Ni.

Chemical additions of 0.2 wt% C and 0.2 wt% C + 1.2% B were introduced into each of the fine silicon powders in order to determine the effect of composition on densification. The type of carbon used was Cabot Monarch 71 which has an average particle size of 160 Å. Elemental boron was purchased from Callary Chemical Co. and had an average particle size of 350 Å. The desired compositions were mixed for 1 hr in a Spex Industries Mixer/Mill (Model 8000-11) using acetone as a dispersion medium.

Carbon was selected because it could enhance the removal of SiO_2 layers on the Si particles by chemical reduction and, consequently, maintain a high surface energy of Si, which drives the sintering process. Boron

was selected as an additive because it has limited solid solubility in Si and may act as a grain growth inhibitor during sintering in the same was that B, MgO and ThO_2 affect grain growth and sintering in β-SiC, Al_2O_3 and Y_2O_3, respectively.

2) Sintering experiments and results

Sintering experiments were performed on powder compacts (5/8" diameter × ¼" thick) of each composition which had been fabricated by isostatic pressing at 30,000 psi. The green density of nearly all specimens was 56% of theoretical. Each specimen was fired in an open Al_2O_3-boat placed inside an Al_2O_3 tube, closed on one end, located inside a Pt-Pt 40% Rh wound resistance furnace. In all cases, the prevailing atmosphere was flowing argon at 2 SCFPH which is first passed through an "oxygen gettering" furnace before entering into the sintering furnace. The partial pressure of oxygen in the sintering furnace is estimated to be $\sim 10^{-8}$atm.

The effect of particle size and composition on the fired density of silicon is shown in Table V. The pure, crystalline silicon powder densifies only a few percent when sintered at 1350°C, a temperature which is about 96% of the melting point. By using a powder having an average particle size of 0.23 μ instead of 1.3 μ, the linear shrinkage increases from 1 to 2.4%. The addition of a small amount of carbon actually decreases the amount of shrinkage from 1 to ∿0% in Powder A; this shrinkage reduction possibly being due to the formation of SiC during sintering. The fired sample did have some strength, indicating that interparticle necks formed. The addition of both boron and carbon to Powder A and Powder B does increase the shrinkage and fired density. There is little change in the amount of densification when the doped or undoped Si powders are sintered at temperatures higher than 1350°C but below a temperature at which any liquid forms. However, Powder B, which contains 0.2% C + 1.2% B, was sintered to greater than 99% of theoretical density at 1391 ± 2°C, a temperature slightly above the eutectic temperature. Considerable densification can, therefore, be achieved by the presence of eutectic liquid. A

TABLE V

Effect of Particle Size and Composition on Density of Silicon Sintered at 1350°C for 1 hr in Ar

Powder	Composition	D_o (g/cc)	D (g/cc)	$\frac{\Delta L}{L_o}$ (%)
Powder A (1.3)	Si	1.28	1.325	1
"	Si+0.2 wt% C	1.30	1.30	0
"	Si+0.2 wt% C+1.2% B	1.31	1.35	1.5
Powder B (0.23)	Si	1.26	1.36	2.4
"	Si+0.2 wt% C	1.27	1.32	1.3
"	Si+0.2 wt% C+1.2% B	1.28	1.43	4

D_o = density of green compact

D = fired density

$\frac{\Delta L}{L_o}$ = linear shrinkage

polished section of the dense, sintered sample, illustrated in Fig. 35, shows 1) a small percentage of large, porous second phase particles (dark grey) which are probably SiC, 2) a large fraction of fine micron-size particles (light grey) which are B_4Si (identified X-ray diffraction) and 3) a few small pores (black spots) about 5 μ in size.

In an attempt to determine if the densification of Si in the solid state is limited by the presence of a SiO_2 layer on the surfaces of the particles, a chemical leaching experiment was done by soaking 0.23 μ Si powder for 1 hr in HF. A rapid reaction occurred as evidenced by froth formation on the surface of the stirred suspension. The powder was washed, filtered, dried, compacted and then sintered at 1350°C for 1 hr in argon. Again, the sample had the same fired density as that prepared from unleached powder. This experiment suggests silicon oxide surface layers are not totally responsible for the limited densification of submicron silicon powder during sintering.

3) Observations on microstructure

The effects of heat treatment and composition on the microstructure of sintered silicon are shown in Fig. 36. The results of sintering Powder B (0.23 μ) have been chosen for representation and are identical in detail to those of Powder A except for a change in scale. Sintered silicon has a microstructure (Fig. 36B) characterized by interconnected pores and interconnected solid in which considerable grain and pore growth have taken place (compare Figs. 36A and 36B). The microstructure of sintered silicon is identical to that previously found for sintered β-SiC containing only excess carbon (section VII-A-3). This is readily apparent when comparing Fig. 37 (a higher magnification of Fig. 36B) with Fig. 31B. Large, pore-free solid regions and large pores are evident in the microstructure of sintered silicon shown in Fig. 37. The dense solid regions have an average size of about 4 μ and have the volume of more than 5,000 of the initial powder particles has been relocated into large pores surrounding the dense solid regions. A polished and chemically etched section of sintered silicon (Fig. 38) reveals that these dense solid regions are polycrystalline.

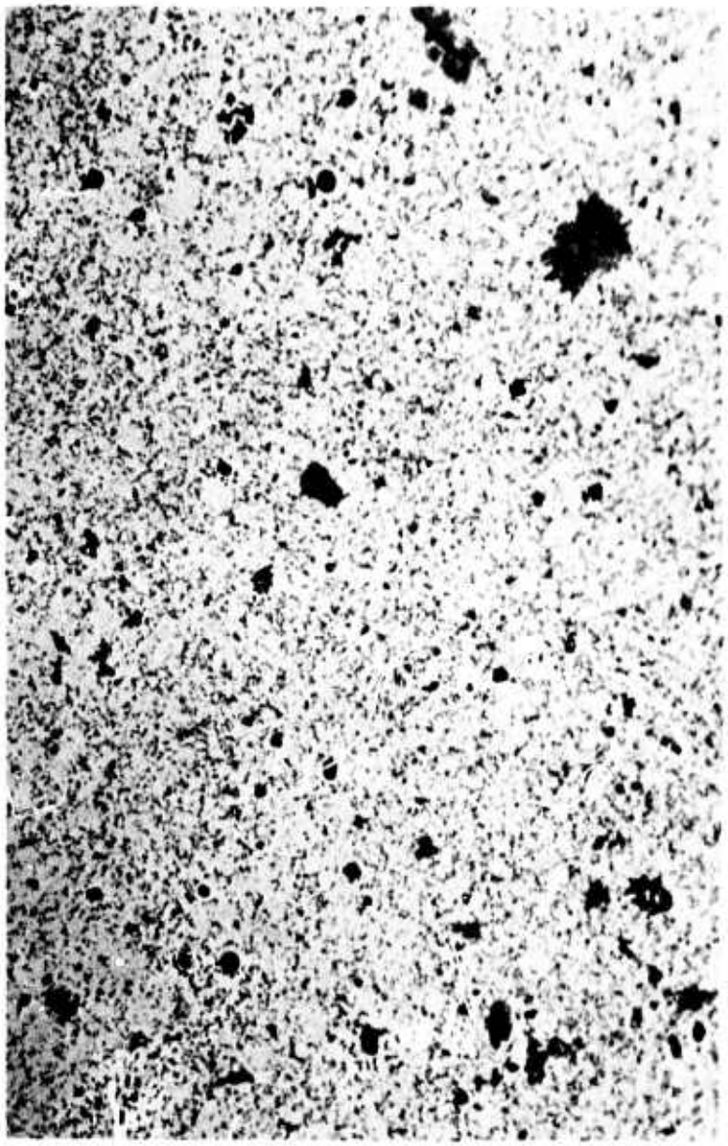

Fig. 35 Microstructure of silicon containing 0.2% C and 1.2% B sintered to 99+% of theoretical density at 1391°C for 1 hr in argon. Reflected light photomicrograph of polished section. 500X

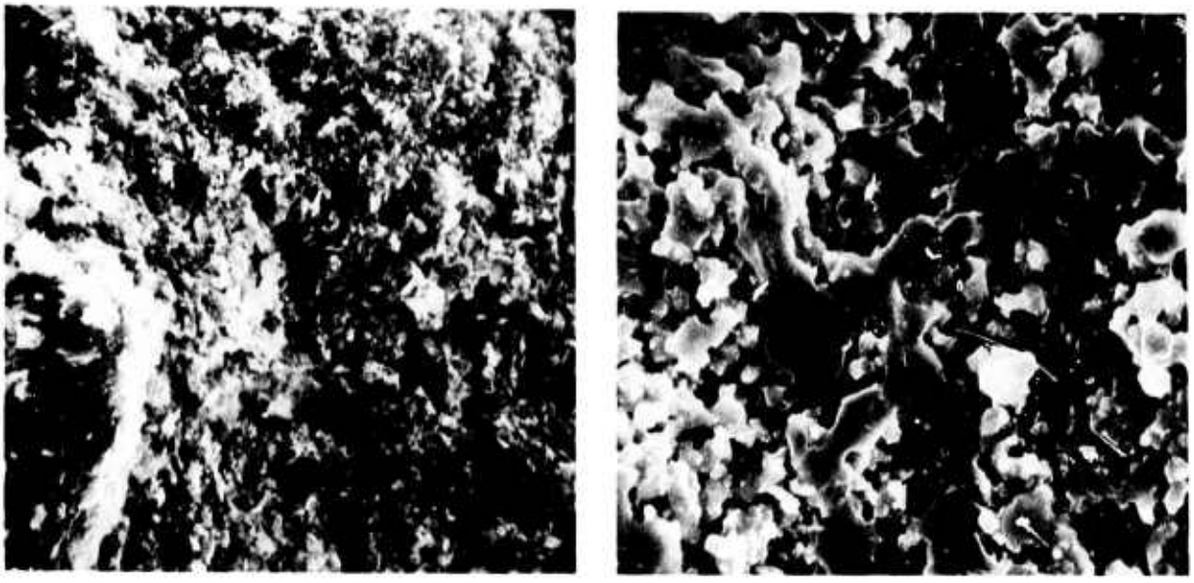

A B

C

Fig. 36 SEM photomicrographs of fractured surfaces of (A) a green compact of silicon before sintering, (B) a sintered compact of silicon and (C) a sintered compact of silicon containing 0.2% C and 1.2% B. Specimens (B) and (C) were sintered at 1350°C for 1 hr in Ar. 1000X

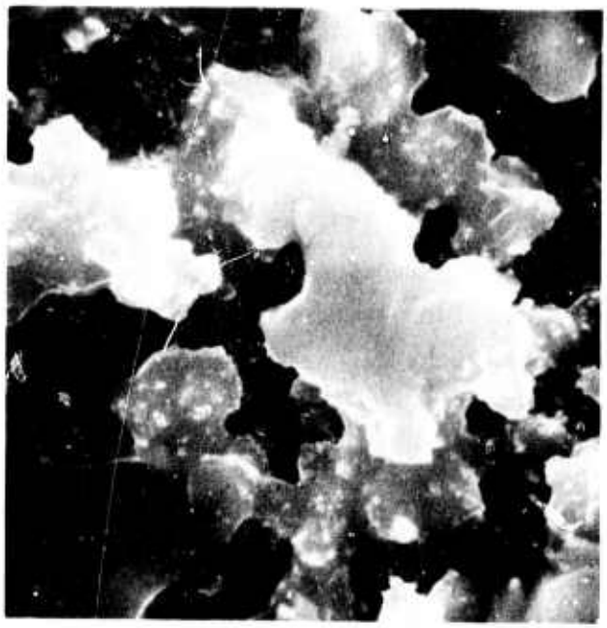

Fig. 37 SEM photomicrograph of a fractured surface of silicon sintered at 1350°C for 1 hr in Ar. 5000X

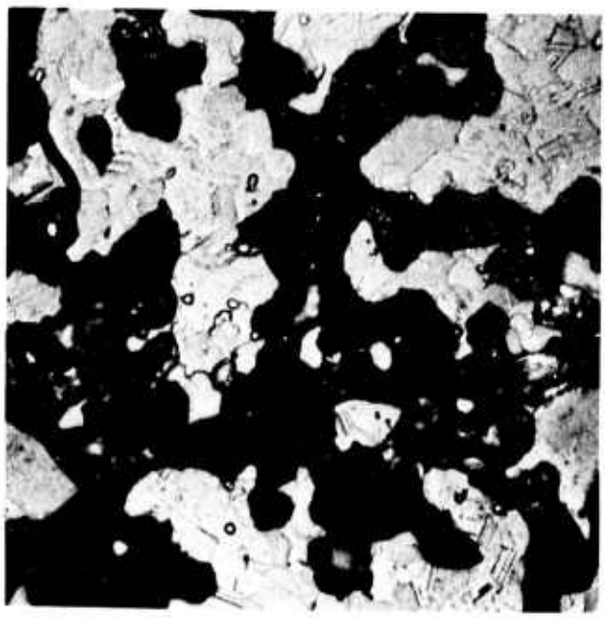

Fig. 38 Reflected light micrograph showing polycrystalline nature of the solid, dense regions developed during the sintering of silicon at 1350°C for 1 hr in Ar. Polished section was chemically etched with mixture of equal parts of HF and HNO_3 at room temperature for 2 seconds.

Addition of both carbon and boron to silicon produces a remarkable change in the microstructure of the sintered body (Fig. 36C). These additions act to generate a fine grain - fine pore structure which permits a greater amount of densification during sintering. These two additions also cause the same microstructure to develop in β-SiC, except that β-SiC powder containing 0.6% B + 0.8% C densifies up to 96% of theoretical density whereas Si powder containing 1.2% B + 0.2% C densifies only to about 62% of theoretical density. The lattice parameters of sintered samples of boron-doped β-SiC and Si decrease from their values for the pure materials, indicating that boron goes into solid solution in both.

C. Preparation and Sintering of Amorphous Silicon Powders

It is desirable to study the effect of average particle sizes less than 0.2 μ and degree of crystallinity on the densification behavior of pure silicon powders during solid-state sintering. Since to our knowledge such fine Si powders with high purity are not commercially available, we prepared our own material by the thermal decomposition of silane, SiH_4, between 600 and 700°C in a gradient furnace. The following reaction takes place:

$$SiH_4(g) \rightarrow Si(s) + 2H_2(g) \; ; \quad \Delta G_{1000°K} = -28.8 \text{ Kcal/mol.}$$

The source of silane was a 4% silane + 96% helium "calibration mixture" produced by the Linde Division of Union Carbide. This gaseous mixture flowed into a fused silica tube located inside the furnace. The silicon powder (or smoke) deposited on the inner wall of the tube. The powder was scraped from the glass wall and characterized by X-ray diffraction, surface area measurements and sintering experiments.

Two experimental runs were made, and powders prepared from these runs are designated Si-1 and Si-2. Si-1 powder was prepared by using a gas flow rate of 0.5 SCFPH and a maximum furnace temperature of 700°C. Si-2 powder was prepared with a gas flow rate of 2 SCFPH and a maximum furnace temperature of 650°C. The color of Si-1 powder was dark brown. Si-2 powder was inhomogeneously brownish-grey in color. Since the powders were prepared in

a temperature gradient furnace, these powders are probably inhomogeneous with respect to particle size, morphology and crystallinity. Therefore, both powders were given an isothermal anneal at 700°C in flowing Ar. After the annealing treatment the color of the Si-1 powder turned light brown while that of Si-2 powder turned dark brown to yellowish brown. X-ray diffraction analysis of these powders showed that Si-1 powder was amorphous in the "as-prepared" form but partly crystallized after the isothermal anneal at 700°C. Preliminary X-ray results on Si-2 powder show it to be partly crystalline in the "as-prepared" state but highly crystallized after the isothermal treatment at 700°C.

Preliminary results of the sintering behavior of these submicron silicon powders are shown in Table VI. An exciting discovery was that Si-1 powder, having a specific surface area of 44 m^2/g (corresponding to 585 Å particles), sintered to 92.3% of theoretical density at 1350°C. At temperatures between 1350 and 1410°C (the melting point of Si) this powder sinters to nearly theoretical density. This finding is highly encouraging for it engenders hope that other "pure" covalent solids can be sintered to densities greater than 90% of theoretical. The microstructure of Si-1 powder sintered to ∿92% of theoretical density is illustrated in Fig. 39. This microstructure is characterized by a fine pore - fine grain structure in which the average pore size and grain size are less than 0.5 μ. This microstructure is nearly identical to that of sintered β-SiC doped with B and C which sinters to relative densities >95%.

Si-2 powder, which has a specific surface area of ∿14.5 m^2/g (∿1760 Å particles), densifies only to a limited extent and shrinks not more than 8% at 1350°C. These sintering results on silicon appear to indicate the extreme importance of starting with a powder of high surface area to obtain high densification of "pure" covalent materials. The results also imply that shrinkage during sintering increases with increasing amorphism of the starting silicon powder. This can be seen from the results listed in Table VII which summarizes the methods of preparation of highly pure silicon powder, state of crystallinity, specific surface area, and the amount of linear shrinkage under constant sintering conditions.

TABLE VI

Specific Surface Area and Sintered Densities of Silicon Powders Prepared from Silane

Powder	S.A. (m^2/g)	Sintering conditions	D_o(%)	D(%)	$\frac{\Delta L}{L_o}$(%)
Si-1, annealed at 700°C	44	1350°C-1 hr	43	92.3	23
Si-2, as prepared	14.6	"	48	61	5
Si-2 + 0.4 wt% B	"	"	"	81	15
Si-2, annealed at 700°C	14.4	"	48	56	7.5

S.A. = specific surface area

D_o = green density of compact

D = fired density

$\frac{\Delta L}{L_o}$ = linear shrinkage

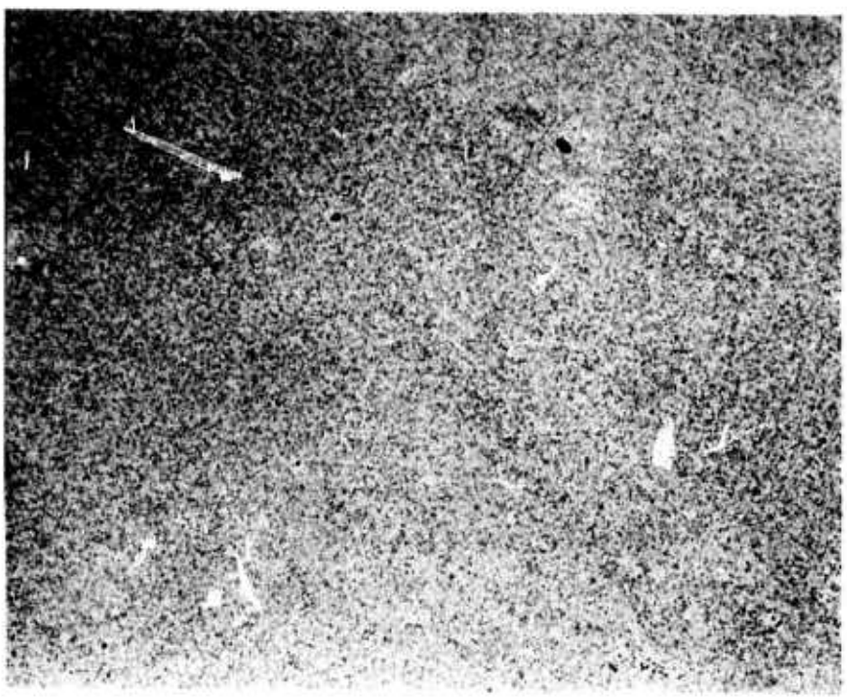

Fig. 39 Microstructure of dense, sintered silicon. 440X

TABLE VII

Powder Characteristics and Sintering Behavior of Silicon

Method of preparation	State of crystallinity	S.A. (m^2/g)	Heat treatment	$\frac{\Delta L}{L_o}$(%)
Jet milling	crystalline	1.9	1350°C-1 hr-Ar	1
"	crystalline	11.4	"	2.5
Decomposition of silane	partly amorphous	14.6	"	8
"	amorphous	44	"	23

An appreciable enhancement in the density of sintered powder of Si-2 type occurs if 0.4 wt% B (this solute concentration is near the solubility limit of B in Si at 1350°C) is added to the starting powder (Table VI). This experiment along with those on the sintering of crystalline silicon powders doped with boron suggest that boron is a densifying additive for both crystalline and amorphous silicon powders and has the greatest effect on fine silicon powders.

Finally, an interesting experimental correlation between percent linear shrinkage and specific surface area of the various silicon powders is illustrated in Fig. 40. There appears to be an approximately linear relationship between these two parameters. Three of the data points fit on a straight line which passes through the origin. One data point falls well off this line. Such a linear relationship can be predicted from sintering theory if the starting powder compacts have a narrow range of green densities and if the pore-grain geometry is such that all pores form an interconnected structure and are intersected by grain boundaries during sintering. From early stage sintering theory $\Delta L/L_o$ is approximately inversely proportional to 1/r, where r is the average particle size. Because 1/r is directly proportional to specific surface area, S.A., a simple linear relationship between $\Delta L/L_o$ and S.A. is predicted.

IX SINTERING OF Si_3N_4

Silicon nitride is a refractory ceramic material with high strength, hardness, high resistance to thermal shock and, consequently, has many potential high temperature applicationssin turbomachinery used in aircraft, ships, trucks, etc. The key to the utilization of this ceramic in such applications is the ability to cheaply fabricate large, complex shapes with high density by a conventional sintering approach. However, pure Si_3N_4 is a primarily covalently bonded solid and is generally classified as "unsinterable". In this section we report on preliminary observations of the sintering behavior and microstructural development at high temperature for two different starting powders of Si_3N_4, one crystalline and the other amorphous.

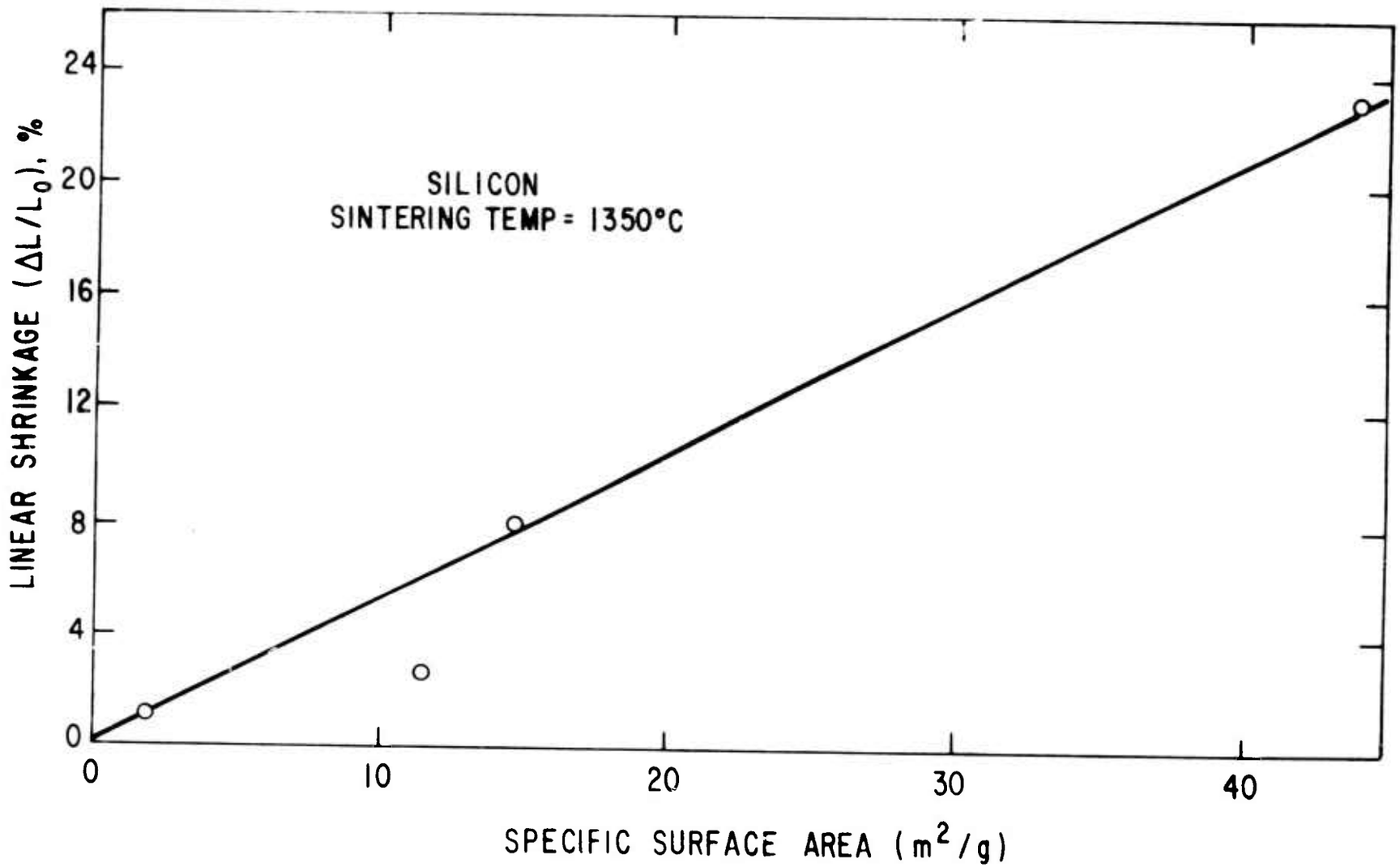

Fig. 40 Linear shrinkage as a function of specific surface area for silicon powders sintered at 1350°C for 1 hr in Ar.

The two types of Si_3N_4 powders investigated were 1) Powder 1 which was the same Plessey Co. powder used in the hot pressing experiments described earlier (section III) and contains 91% α-Si_3N_4 + 9% β-Si_3N_4 particles with a specific surface area of 9.4 m^2/g and with major impurities being $\sim$1.4 wt% O and $\sim$0.1 wt% Fe and 2) Powder 2 which was an amorphous powder synthesized in our laboratory and had a specific surface area of 28 m^2/g and major impurities of oxygen and about 2% free silicon. The particle size and morphology of Powder 2 is shown in Fig. 41. Powder 1 has the same characteristics except for a larger particle size.

A summary of the sintering behavior as well as weight loss data for Si_3N_4 Powders 1 and 2 is illustrated in Table VIII. Powder 1 has a lower specific surface area and a higher relative green density in compact form than Powder 2, but exhibits essentially no shrinkage or densification at temperatures as high as 1820°C in 1 atmosphere of flowing nitrogen. On the other hand, compacts of Powder 2 undergo about 3% linear shrinkage at 1600°C and little shrinkage thereafter even when the temperature is increased to 1820°C. A considerable weight loss occurs for Si_3N_4 above 1700°C and reaches values as high as 6% for Powder 1 and 9% for Powder 2 at 1820°C for a one hr hold period. The higher shrinkage and weight loss exhibited by Powder 2 may be associated with its smaller initial particle size but the possible effect of impurity differences can not be disregarded.

SEM photomicrographs (Fig. 42) and X-ray diffraction analysis of sintered material made from both powders show that for temperatures up to 1700°C, the grain structure is composed of nearly equiaxed grains of primarily α-Si_3N_4. Upon heat treatment at 1820°C, a major microstructural transformation takes place whereby acicular grains with an aspect ratio of approximately 4:1 consume the entire matrix of the fine, equiaxed grains (Fig. 42B). These acicular grains are about 2 microns in length and have been identified as β-Si_3N_4. All grains are well-faceted which is indicative of the attainment of geometrical equilibrium for the grain structure.

The nearly nondensifying nature of Si_3N_4 powders is believed to be related to the formation of β-Si_3N_4 grains with a large aspect ratio that

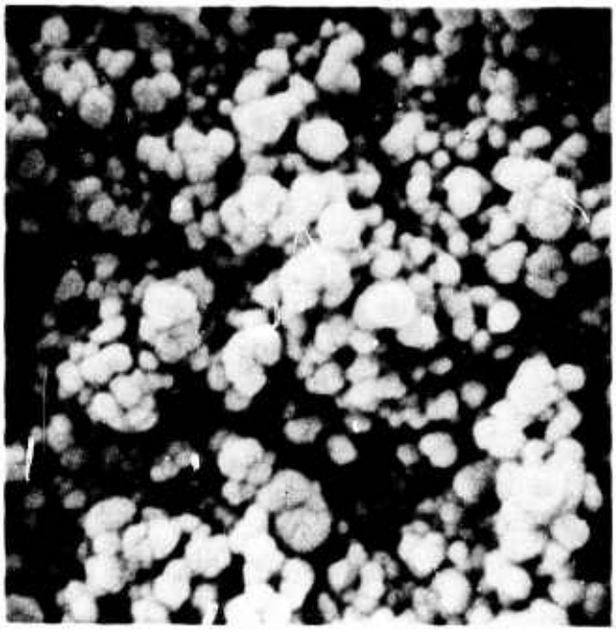

Fig. 41 SEM photomicrograph of Si_3N_4 Powder I showing shape, size, and aggregation of the particles.

TABLE VIII

Sintering of Si_3N_4 for 1 Hr in Flowing N_2

Powder	S.A. (m^2/g)	D_o (%)	D(%)	$\frac{\Delta L}{L_o}$(%)	$\frac{\Delta W}{W_o}$(%)	T(°C)
1	9.4	53	53	0	0.9	1600
1	"	"	52	0	4	1700
1	"	"	52	0	6	1820
2	28	38	42	3	1.8	1600
2	"	"	44	3.5	6.5	1700
2	"	"		4	8.8	1820

S.A. = specific surface area of the starting powder

D_o = relative green density

D = relative fired density

$\frac{\Delta L}{L_o}$ = shrinkage

$\frac{\Delta W}{W_o}$ = weight loss

A

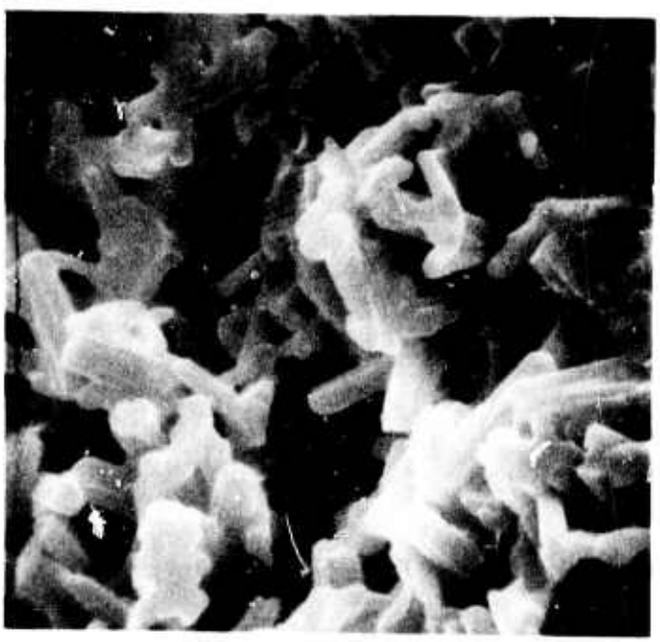

B

Fig. 42 SEM photomicrographs of fractured surfaces of sintered Si_3N_4 Powder I. (A) Sintered at 1700°C for 1 hr in N_2, (B) sintered at 1920°C for 1 hr in N_2. 5000X

rigidify the structure so that very little macroscopic shrinkage or densification may take place. This observation in Si_3N_4 powders is similar to the sintering behavior of Powder II of β-SiC in which it is observed that densification essentially ceases when large α-SiC plates rapidly grow in the fine grained β-SiC matrix (see section VII-B). It is rationalized that grain boundaries in grain structures composed of grains with a large aspect ratio do not act as effective sources of matter which can be deposited into the pore space to cause densification.

X SINTERING OF AlN

A few sintering experiments were performed on two AlN powders of nearly the same specific surface area (∿3 m^2/g), one purchased from Atomergic Chemical Co. and the other from Alpha Inorganics (VENTRON). Green compacts with relative densities ∿60% were fired at temperatures up to 2000°C in one atmosphere of flowing nitrogen. Both of these powders exhibit approximately 2 to 4% of linear shrinkage over the temperature range of 1800 to 2000°C. Scanning electron microscopy photomicrographs of the microstructure of the sintered AlN show that grain and pore growth occur at the temperatures investigated. Furthermore, the grains are equiaxed indicating no restriction on densification due to the effect of large aspect ratios of the growing grains. This finding suggests that the limitation of densification of these AlN powders may be due to large (∿0.6 μ) initial particle size and/or impurity effects.

XI SINTERING OF B_4C

A. Introduction

Boron carbide is one of the compounds suitable for the investigation of the sintering phenomena in covalent solids because:

1) The study of bonding and bond lengths in B_4C justifies this material to be classified as a typical covalent solid.

2) In contrast with silicon carbide, which is believed to have an extremely narrow region of nonstoichiometry, B_4C is known to have a wide region of nonstoichiometry covering at least the compositional interval from $B_{13}C_2$ to $B_{12}C_3$. Consequently, it may be a useful model material for the investigation of the effect of structural defects in covalent solids.

3) It is a very stable compound with a low vapor pressure up to the melting point, which makes it particularly attractive for sintering experiments.

4) B_4C ceramic is now being fabricated exclusively by hot pressing. It has several important applications due to its hardness, low specific weight, high thermal conductivity and neutron absorption properties. Thus, new information on its sintering may be of technological interest.

The objective of the following paragraphs is to describe introductory sintering experiments performed with B_4C in order to determine whether or not it can be successfully sintered without using pressure. We will not review the complex crystal chemistry of B_4C and the yet not fully understood phase relations in the boron-carbon system.

B. Powder Specifications

B_4C from two different sources was procured and characterized by spectrographic analyses. Oxygen and nitrogen were determined by vacuum fusion and surface area by low temperature nitrogen adsorption.

Specimen No. 1: B_4C - Poly Research Corporation, New York
Cat. No. B-315, specified as 99.9% pure, -325 mesh.

Specimen No. 2: B_4C - Grade HP - Boride Products, Inc., Michigan
Specified as 99.0% pure with Fe, Mg and O as main impurities, submicron particle size.

The first powder was grey, highly crystalline and too coarse for sintering experiments. Therefore, a -5 μm particle size fraction was separated by sedimentation from an aqueous dispersion. The chemical composition given in Table IX refers, however, to the original specimen. The response of

TABLE IX

B_4C Powder Characteristics

Sample	B_4C-1	B_4C-2	B_4C-2 calcined at 1450°C
Composition %:			
C	21.9	21.1	22.9
N	n.d.	0.3	0.3
O	0.21	4.4	0.55
Fe	0.09	1.0	1.0
Mg	<0.01	2.0	2.1
Ti	n.d.	0.002	n.d.
Al	n.d.	0.02	n.d.
Si	0.11	n.d.	<0.05
B/C Molar Ratio	3.94	-	3.57
Specific Surface Area m^2/g	1.6	17.2	16.1
Density	2.48	n.d.	n.d.

this powder to sintering was, in general, not favorable as shown in Table X.

The powder from the second source had a specific surface area corresponding to 0.08 μm average particle size. The morphology of its particles is shown in Fig. 43, which also demonstrates the very wide crystallite size distribution. The striations seen in some of the particles are probably stacking faults. The aggregates of very fine particles could be free carbon which also has been detected by electron diffraction. As shown in Table 1X, the purity of this powder is much less than specified by the supplier. The high oxygen content, however, can be reduced to an acceptable level of 0.5% by calcination of the powder at 1450° in 100 Torr argon for one hour.

The high magnesium content is obviously the result of the preparation technique which uses reduction of B_2O_3 by Mg metal in the presence of carbon.

Mg has been recently claimed to be an effective sintering aid in densification of B_4C (U.S. Pat. No. 3.749571 of July 1973) see also T. Vasilos and S. K. Dutta, Bull. Amer. Cer. Soc., Vol. 53, 453 (1974). This impurity has not been considered deleterious.

C. Processing and Sintering

For preparation of the sintering specimens, the powders were dispersed in a 1/2% benzene solution of an organic pressing aid and in some experiments, 50g batches were milled 5 hrs by 3/16" cemented carbide balls in plastic containers. The dispersion was then dried and the powder screened through a 60-mesh sieve. Die pressing of 2 g pellets at 6000 psi yielded a green density of about 60% of the theoretical -2.54 g/cc.

In the course of this investigation, additions were made to B_4C in hope of aiding its sintering. For this purpose, two compounds were selected: SiC and Be_2C. The first was chosen as a species which was expected to bring about liquid formation at high temperature and hence aid densification via liquid assisted sintering. This choice was essentially an extension of observation of sintering in the system SiC-B_4C (see S.M. Billington, J. Chown, A.E.S. White in "Special Ceramics", P. Popper, ed., Vol. 2, 1962).

Be_2C on the other hand, was chosen as a species which was not expected

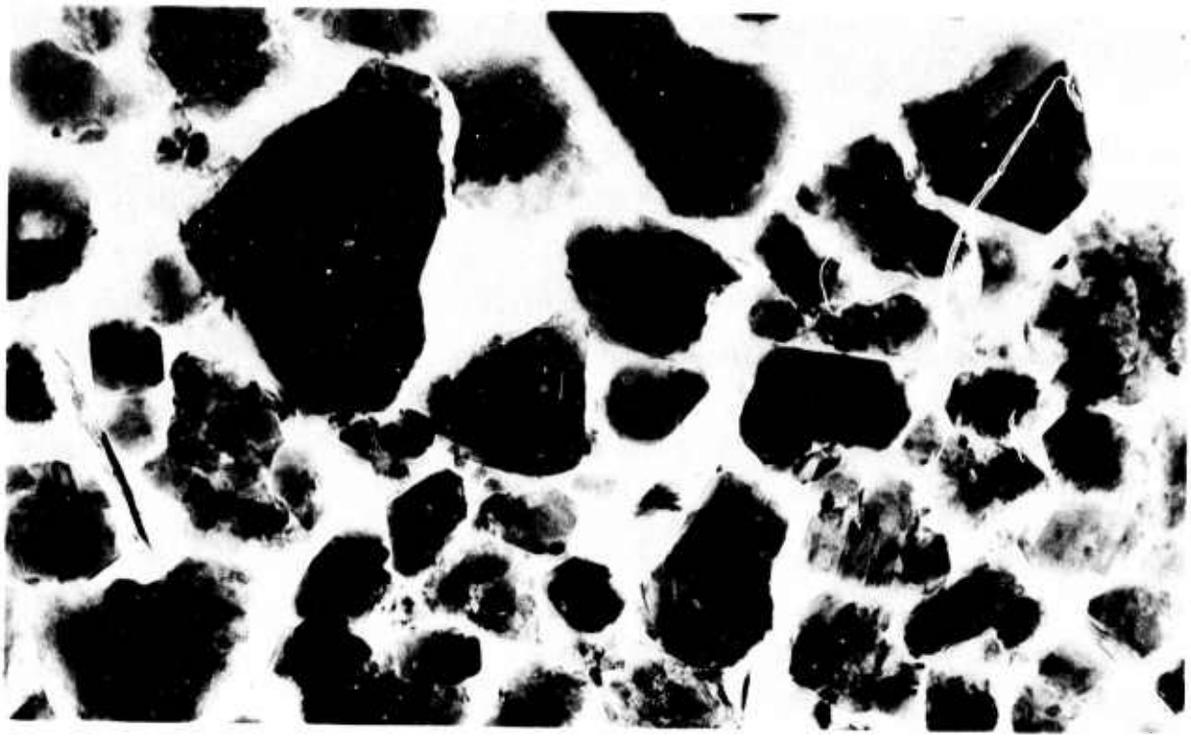

Fig. 43 Boron carbide, grade HP from Boride Products, Inc. TEM, 38,400X

to bring about liquid formation when added to B_4C in small amounts. The choice of the additions was made without knowledge of the high impurity content of B_4C which may have changed the phase relations considerably.

Elemental boron was added to all compositions made from powder 2, calculated so as to compensate for the hyperstoichiometric carbon determined by analysis (Table IX). For this purpose Elemental Amorphous boron, obtained from Callery Chemical Co., Pa. (Tech. Bulletin, No. C-1400) was used.

The compacts were sintered in a high-temperature carbon element resistance furnace at temperatures between 2100° and 2300°C in flowing argon or argon-nitrogen atmospheres. Commercial high purity gases were used with oxygen content less than 10 ppm as determined by the supplier. The furnace and its performance has been described previously (P. D. St. Pierre, M. J. Curran, G. E. TIS Rept. 72CRD012, Dec. 1972).

Temperature measurement was done with an L&N pyrometer by directly viewing the sintering object. The pyrometer was calibrated at the melting point of a saphire single crystal, i.e., at 2050°C. No other corrections, such as for emissivity or reflectance of the viewing part were considered. The reading is believed to be accurate to within ±25°C; the main source of uncertainty arising from occasional slight fogging of the window.

The density of the sintered specimen was determined by liquid displacement and metallography was done after sectioning, polishing and electrolytic etching in 10% KOH.

The results in terms of density and fractional density based on theoretical specific weight 2.54 g/cc are summarized in Table X.

D. Results

In the series of experiments 1 to 3 done with powder 1 , there was little sintering, even at temperatures close to where melting occurred. Melting was probably due to the contact with carbon, which resulted in the formation of a eutectic between B_4C and C. (The eutectic temperature is

TABLE X

Summary of Sintering Experiments with B_4C

Exp. No.	Powder No.	Addition % by wt.	Sint. Temp. °C	Final Density g/cc	Final Density %	Shrinkage %	Comment
1	1	none	2100	1.55	61.8	nil	
2	1	none	2300	1.60	63.5	1.5	
3	1	none	2350+	-	-	-	melting
4	2	none	2120	1.65	65.5	4.2	
5	2	none	2260	1.81	71.9	6.6	
6	2	0.5 Be_4C	2130	2.05	81.6	9.4	
7	2	1.0 Be_4C	2130	2.01	80.1	8.9	
8	2	same	2230	2.14	85.5	11.0	
9	2	same	2280	2.38	94.0	16.5	
10	2	same	2300+	-	-	-	partial melting
11	2	1% SiC	2150	1.96	77.8	n.d.	
12	2	10% SiC	2150	2.07	80.6	n.d.	
13	2	1% SiC	2300+	2.37	93.6	n.d.	melting in contact with setter

somewhat uncertain and has been placed by various authors anywhere between 2200 and 2400°C. More recent investigations agree on the high region of this interval (see for instance R. Kieffer, et al., Ber. Dt. Ker. Ges. 48, 385 (1971)). However, shrinkage and some indication of densification has been detected in this relatively pure and coarse B_4C powder.

The finer powder, no. 2 (which also contains appreciable amounts of Mg and Fe) responds to the same sintering conditions by more densification. A density 72% could be obtained at 2260°C. It is, of course, not possible at this point to determine whether the enhanced densification was due to the fine particle size or the impurities in this powder.

An addition of Be_4C to powder 2 further provides densification; there was essentially no difference in the effect of 0.5 and 1% addition. At 2260°C, in 30 minutes a density of 2.38 g/cc (corresponding to 94% of the theoretical) was obtained in two experiments. This was the highest degree of sintering achieved in this investigation. At still higher temperature, melting occurred at the contact of the pellet with the carbon boat.

Figure 44 shows the as-polished section of specimen No. 8 sintered to 85% of theoretical density at 2230°C. Figures 45 and 46 give the as-polished and etched appearance of specimen no. 9 which yielded the highest density. The microstructure shows large, equiaxed grains, approximately 300 μm in diameter, and large rounded off closed pores mainly at the grain boundaries. Some small spherical pores have been obviously trapped in the growing grains. There are also small grains of a second phase distributed near grain boundaries.

A 1% SiC addition to B_4C also brought about enhancement of densification at 2150°C. The degree of densification was somewhat increased where the addition was increased to 10%, however, the difference is only marginal. At 2300°C a density of 2.37 g/cc was obtained corresponding to 93.6% of the theoretical (Fig. 47). At this temperature, however, partial melting occurred due to interaction with the carbon setter.

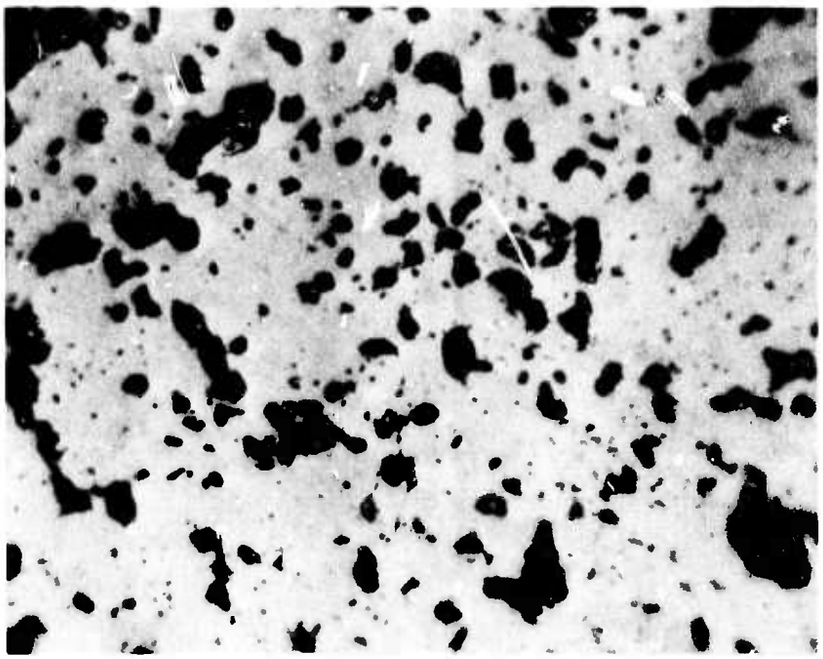

Fig. 44 B_4C sintered with 1% Be_2C at 2230°C in argon to 85% density. As-polished section. 500X

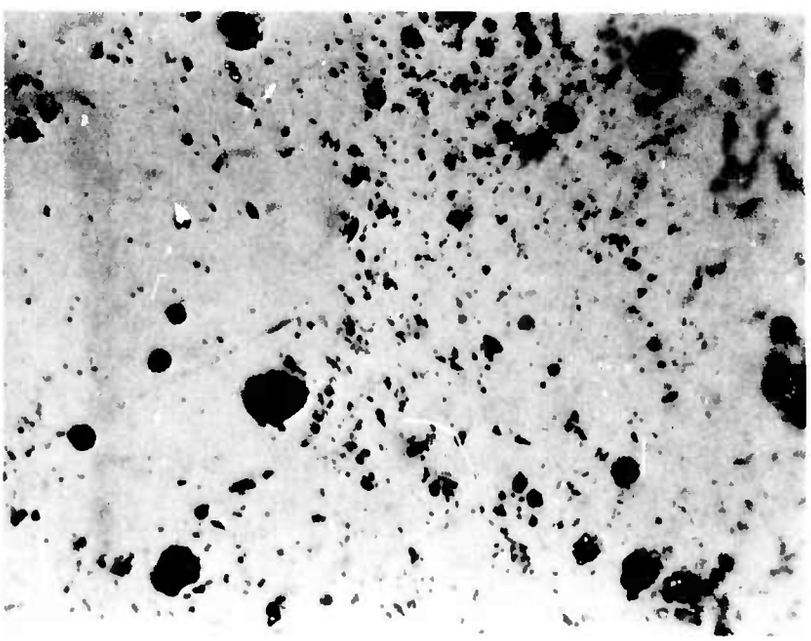

Fig. 45 B_4C sintered with 1% Be_2C at 2280°C in argon-nitrogen atmosphere to 94% theoretical density. As-polished specimen. 500X

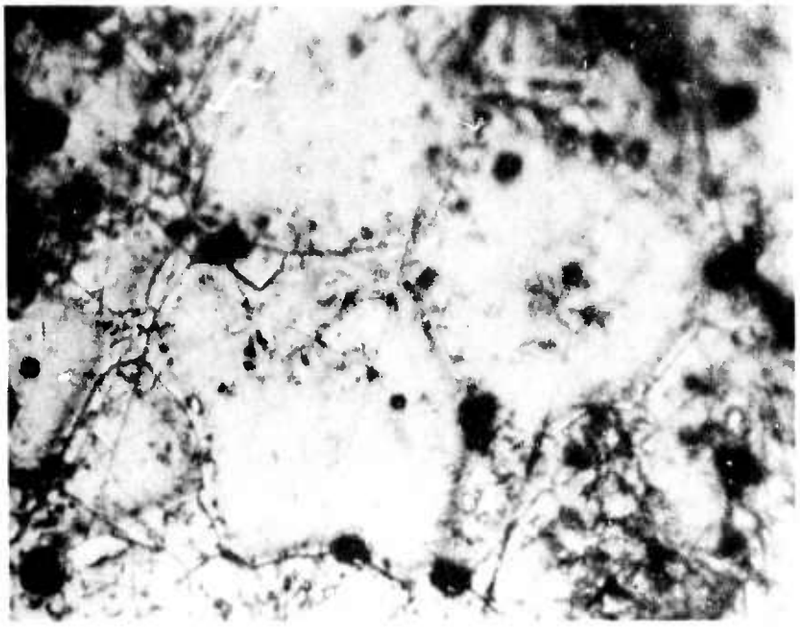

Fig. 46 Same specimen as Fig. 44, electrolytically etched in KOH.

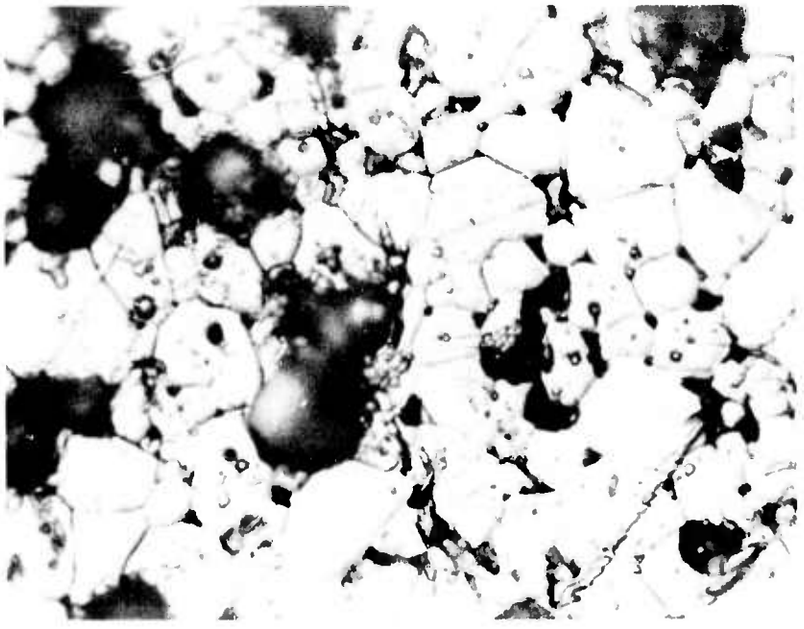

Fig. 47 B_4C sintered with 1% SiC at 2300°C in argon to 93.6%. 500X

E. Conclusion

It has been shown that submicron B_4C is amenable to sintering to relatively high densities in the presence of Be_2C or SiC. Whether or not the impurities contained in the powder, i.e., Fe and Mg also assisted the sintering process has not been established. Sintering was observed to occur above 2100° and the highest density was obtained only close to the temperature where melting occurred in contact with carbon. The highest density achieved was 94% of the theoretical.

Thus, it appears that B_4C is a promising material for study in an investigation of sintering in covalent solids. It also appears that further study of sintering in B_4C may result in a practical process amenable to B_4C ceramic part fabrication.

XII CONCLUSIONS FROM SINTERING STUDIES

In consideration of the observations on microstructure development during firing of powders of covalently bonded solids given above, it is apparent that a distinction must be made between the phenomenon of macroscopic shrinkage and consequent densification of a powder compact, commonly called "sintering", and that of microscopic densification coupled with porosity restructuring, which can result in little or no macroscopic shrinkage and densification. It has been proposed that previously observed inability to "sinter" powders of pure, covalently bonded solids (meaning the absence of appreciable macroscopic densification) occurred for reasons such as too high a grain boundary energy or too low a volume diffusion coefficient, which imply the general absence of microscopic densification and hence the "absolute" unsinterability of this class of solids. It may be concluded from the work reported here that such explanations are oversimplified, and at most, only partly correct.

Powder compacts of pure β-SiC and Si, archetypical covalent solids, develop identical microstructures on firing. These consist of theoretically dense regions, having the volume of thousands of the initial powder particles,

connected to each other at a few points and separated by large pores. The existance of such dense regions and the large dihedral angles also observed mean that the grain boundary energy is not so high as to preclude the formation and growth of many necks between particles. That some relative particle orientations giving rise to high energy grain boundaries may exist is, however, implied by the fact that a hot pressed piece of β-SiC changes its structure on annealing by shrinking some grain boundaries and thus breaking contacts. In balance, though, lack of macroscopic densification does not appear to be the result of a high grain boundary energy.

The mechanism by which the characteristic microstructure of fired compacts of pure β-SiC and Si powders develops is proposed to be the following: on heating the compact, necks form between the powder particles and grow as a result of surface diffusion of matter over the particle surfaces to the neck region. The grain boundary formed between particles is mobile and can sweep through the smaller particle and thus be eliminated. The resulting single grain, under the influence of capilarity forces, then attempts to reduce its surface area by assuming a more compact shape. This results in a stress on the necks attaching that grain to others. If some necks at this stage, or at the very beginning, contain high energy grain boundaries they may shrink under the influence of this or other stresses. The net result of this process, which is similar to that proposed by Greskovich and Lay to explain grain growth in compacts of oxide powders[16] is the aggregation of a group of particles into a dense, solid region composed of grains which are larger than the original powder particles and separated by relatively low energy grain boundaries.

This process leads only to localized densification, as observed in the microstructures, since the pore volume included between the original powder particles has only been redistributed and moved out to the surface of the dense region. Thus there is little macroscopic shrinkage of the powder compact. In order for that to occur there must be matter transport from the grain boundaries to the pores by volume diffusion and/or grain boundary diffusion.

This proposed mechanism postulates that the characteristic microstructure of nonsintering, pure β-SiC and Si develops as a result of a greater transport of matter by surface diffusion than by volume or grain boundary diffusion. Once the structure forms, macroscopic shrinkage resulting from volume or grain boundary diffusion can proceed at only a negligible rate because the number of grain boundaries that can act as matter sources for filling pores (those boundaries in the necks connecting the dense regions) are relatively few. Also, shrinkage requires a coordinated shape change of grains to fill the surrounding porosity and this is much more difficult to accomplish with a large, polycrystalline dense region surrounded by large pores than with small grains surrounded by small pores.

The explanation is consistent with the observation that one of the additives which makes β-SiC sinterable (B) also slows down the rate at which the surface area of a powder compact decreases during firing at lower temperatures. This implies that surface diffusion is retarded and hence grain growth reduced, thus preventing the generation of a microstructure for which shrinkage is difficult. It is also consistent with the observation that a compact of ultra-fine, pure Si powder will sinter to almost theoretical density without additives because, by decreasing powder size, diffusion distances are shortened, and due to higher curvatures, higher effective stresses exist at the pore/solid interfaces. Both of these increase the relative porportion of matter transport by volume or grain boundary diffusion compared to that by surface diffusion.

Another factor also appears to retard macroscopic shrinkage in β-SiC and α-Si_3N_4. That is the growth of grains of another phase having a high aspect ratio in the powder compact. These prevent the removal of porosity by interfering with the necessary coordinated change in grain morphology that must occur during shrinkage.

Generalizing from the work already done, the following tentative conclusions may be made and serve as working hypotheses to guide further work:

1) Covalent solids are not intrinsically unsinterable.

2) Powder compacts of these materials may be caused to shrink macroscopically if:

   a. growth of second phase crystallites having a high aspect ratio is avoided;

   b. an ultra-fine particle size is used; or

   c. an additive is employed which slows down surface diffusion so that there is a high proportion of matter flow by volume or grain boundary diffusion compared to surface diffusion.

REFERENCES

1. Supplied through the courtesy of Dr. Joseph Gebhardt, General Electric Re-Entry and Environmental Systems Division Pyrolytic Materials Facility, Philadelphia.

2. A. F. McLean, E. A. Fisher and R. J. Bratton, "Brittle Materials Design, High Temperature Turbine." AMMRC CTR74-26, Interim Report, April 1974.

3. A. F. McLean, E. A. Fisher and R. J. Bratton, "Brittle Materials Design, High Temperature Gas Turbine." AMMRC CTR73-72, Interim Report, September 1973.

4. G. G. Deeley, J. M. Herbert and N. C. Moore, "Dense Silicon Nitride," Powder Met. 8, 145-51 (1961).

5. J. T. Gray, "The Defect Solid State," Interscience Publishers, New York, p. 346.

6. R. W. Davidge, A. G. Evans, D. Gilling and P. R. Wilyman, "Oxidation of Reaction-Sintered Silicon Nitride and Effects on Strength," Special Ceramics, Vol. 5. Proceedings of the 5th International Symposium on Special Ceramics, held by the BCRA, Stoke-on-Trent, England, 14-16 July 1970. Edited by P. Popper. Manchester, England: British Ceramic Research Association (1972) 329-44.

7. Powder supplied through the courtesy of Mr. William Flock.

8. J. H. Rosolowski and C. D. Greskovich, "Ceramic Sintering," Semi-Annual Technical Report, General Electric Co., SRD-74-116, Contract N00014-74-0331, Advanced Research Projects Agency.

9. S. Prochazka and P. Smith, "Investigation of Ceramics for High-Temperature Turbine Vanes," Final Report, General Electric Co., SRD-74-040, Contract N00019-72-0129, Naval Air Systems Command.

10. G. Busch and H. Labhart, "Uber bed Mechanismus ber Elektrischen Leit-Fahigkeit des Silicium Carbids," Helv. Phys. Acta 19, 463 (1946).

11. J. A. Lely and F. A. Kroger, "Electrical Properties of 6H-SiC Doped with N, B or Al" in Halbleiter und Phosphore (1958) p. 525.

12. H. J. van Daal, C. A. A. J. Greebe, W. F. Knippenberg and H. J. Vink, "Investigations on Silicon Carbide," J. Appl. Phys. 32, 2225-33 (1961).

13. H. D. Batha and L. H. Hardy, in Silicon Carbide - 1973. R. C. Marshall et al eds., University Press, S.C., 1974.

14. Handbook of Electronic Materials, Vol. 5, Plenum Press (1971) p. 56.

15. S. Prochazka, C. A. Johnson and R. A. Giddings, "Investigation of Ceramics for High-Temperature Turbine Components," Quarterly Progress Report No. 2, Contract N62269-75-C-0122, April 1975.

16. C. Greskovich and K. W. Lay, "Grain Growth in Very Porous Al_2O_3 Compacts, J. Amer. Ceram. Soc. 55, 142-46 (1972).

17. F. A. Nichols and W. W. Mullins, "Morphological Changes of a Surface of Revolution Due to Capillarity-Induced Surface Diffusion," J. Appl. Phys. 36, 1826-35 (1965).

18. J. H. Rosolowski and C. Greskovich, "Theory of the Dependence of Densification on Grain Growth During Intermediate Stage Sintering," J. Amer. Ceram. Soc. 58, 177-182 (1975).

19. A. Kuper, H. Letaw, L. Slifkin, E. Sonder and C. T. Tomizuka, "Self-Diffusion in Copper," Phys. Rev. 96, 1224-25 (1954).

20. R. L. Coble, "Sintering Crystalline Solids. II. Experimental Test of Diffusion Models in Powder Compacts," J. Appl. Phys. 32, 793-99 (1961).

21. T. E. Clare, "Sintering Kinetics of Beryllia," J. Amer. Ceram. Soc. 49, 159-65 (1966).

22. S. Prochazka and R. M. Scanlan, "Effect of Boron and Carbon on Sintering of SiC," J. Amer. Ceram. Soc. 58, 72 (1975).